東海大學畜產與生物科技學系

Department of Animal Science and Biotechnology

Tunghai University

碩士論文

Master Thesis

指導教授：歐柏榮博士

Advisor: Bor-Rung Ou, Ph.D.

利用抑肌素基因 5 端調節區建立篩選調節抑肌素基因表現之中草藥分子生物分析平台

Establishment of molecular biological assay system for screening myostatin inhibitor in Chinese herbs

研究生：黃鈴雅

Graduate student: Ling-Ya Huang

中華民國一百零八年六月二十一日

June 21, 2019

TABLE OF CONTENTS

LIST OF FIGURES

LIST OF TABLES

ACKNOWLEDGEMENT

I would like to express my deep gratitude to Professor Bor-Rung Ou of the Animal Science and Biotechnology at Tunghai university. The accompany of Doctor Ou was always there whenever I ran into a trouble spot or had a question about my research or writing. He consistently allowed this paper to be my own work, but steered me in the right the direction whenever he thought I needed it.

I would also like to thank the experts who were involved in the validation survey for this research project: Professor Jan-Ying Yeh, Professor Yu-Chuan Liang. Without their passionate participation, the validation survey could not have been successfully conducted. I appreciate Professor Chu-Liang Chen helping me, when I stocked in my research or writing.

I would also like to acknowledge lab seniors: Chih-Long Shen, Yan-Shun Lee, Kevin Wang, Joyce Chang-Liao and Wilson Huang. And I also appreciate Mimi Chen, Liang-En Yu, Michelle Tai giving me encourage when I am in low. I am gratefully indebted to them for their very valuable comments on this thesis.

Finally, I would like to thank all those good human beings, whom I have come across in this path of my journey. They provide me with unfailing support and continuous encouragement throughout my years of study and through the process of researching and writing this thesis. This accomplishment would not have been possible without them. Thank you.

Author

Ling-Ya Huang

ABSTRACT

Myostatin, also known as growth and differentiation factor 8 (GDF-8), is one of the major regulators of skeletal muscle development. The phenotypes of myostatin-mutant cattle and mice have clearly established myostatin as a negative regulator of skeletal muscle growth. It has been found that the growth rate of myoblasts cultured in serum from double-muscled cattle fetuses was higher than myoblasts in normal-muscled cattle fetuses serum. Deletion and inhibition of myostatin in animals lead mainly to increased muscle mass and reduced fat mass. It is important to find an efficient way to regulate myostatin activity to improve animal growth. Myostatin 5'-regulatory region was used to construct the reporter plasmid. L8 rat myoblasts were transfected with reporter plasmids. After selection, transfected L8 cells were used to screen the CMH (Chinese medicine herbs) with myostatin regulators. Twenty seven CMHs were examined by using this molecular biological screening assay. Four CMHs were identified containing the myostatin regulators. It is concluded this molecular screening system is useful to identify CMH containing myostatin regulator.

LITERATURE REVIEW

Myostatin

Introduction of myostatin

Myostatin, also known as growth and differentiation factor 8 (GDF-8), is one of the major regulators of skeletal muscle development (Beyer *et al*., 2013). It is a member of the transforming growth factor-β (TGF-β) superfamily. Myostatin plays a negative regulator in skeletal muscle growth. Overexpression of myostatin induces skeletal muscle atrophy and the mutations in the myostatin-encoding region are response for muscle hypertrophy and hyperplasia (Swatland and Kieffe, 1974). The phenotypes of myostatin-mutant cattle and mice have clearly established myostatin as a negative regulator of skeletal muscle growth. It has been found that the growth rate of myoblasts cultured in serum from double-muscled fetuses was higher than myoblasts in normal-muscled serum (Gerrard and Judge, 1993). Furthermore, addition of myostatin to culture medium inhibits the proliferation of myoblasts (Thomas *et al*., 2000; Rios *et al*., 2001; Taylor *et al*., 2001). Moreover, the degree of inhibition is dose dependent and reversible (Thomas *et al*., 2000).

Activation of the myostatin and effect of myostatin on muscle development

Myostatin protein is predominantly synthesized in skeletal muscle as a 375-amino acid protein. It is proteolytically processed and then mature C-terminal myostatin is secreted. Pro-myostatin dimerizes by a disulfide bond near the caboxy(C)-terminus and is systematically cleaved at the RSRR (Arg-Ser-Arg-Arg) site by a calcium-dependent serine proteinase, which was known as furin convertase. (Molloy *et al*., 1994, 1999; Lee and McPherron, 2001). This proteolysis generates the N-terminal propeptide and a C-terminal receptor-binding domain (McFarlane *et*

al., 2005). The latent myostatin complex forms as the propeptide noncovalently binds the C-terminal region, and this prevents myostatin from binding to the target receptor (McFarlane *et al*., 2005). Members of the bone morphogenetic protein-1/tolloid (BMP-1/TLD) family are metalloproteinases that can cleave the propeptide and release mature myostatin (Figure 1) (Wolfman *et al*., 2003). Mature myostatin binds to type IIB receptor and mainly transduces the signal via the Smad pathway (

Figure 2). Among mammals, myostatin gene contain 3 exons and the myostatin gene among different species are highly homologous, indicating a conserved function (Table 1) (Lee and McPherron, 2001; Shen, 2010). Myostatin appears to down regulate both prenatal and postnatal myogenesis (Deveaux *et al*., 2001; Pirruccello-Straub *et al*., 2018). In the previous research shows that myostatin down regulates the muscle fiber number by reducing the myoblast proliferation and differentiation during early myogenesis (Deveaux *et al*., 2001). Myostatin appears to be a target for compensatory muscle growth in farm animals, and for muscle wasting and cachexia in illness (Pirruccello-Straub *et al*., 2018).

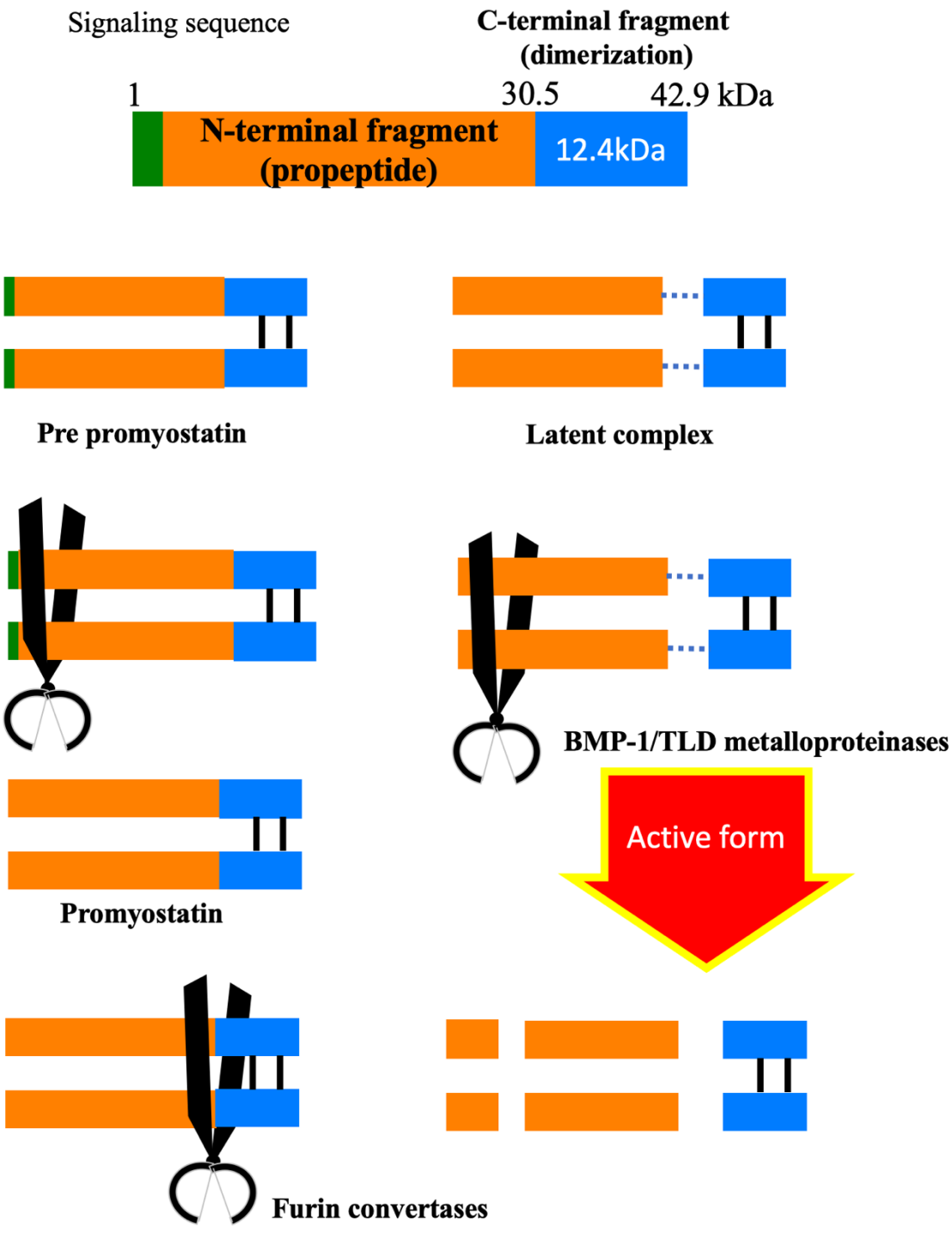

Figure 1. The activation of myostatin by furin convertase and BMP-1/TLD metalloproteinase

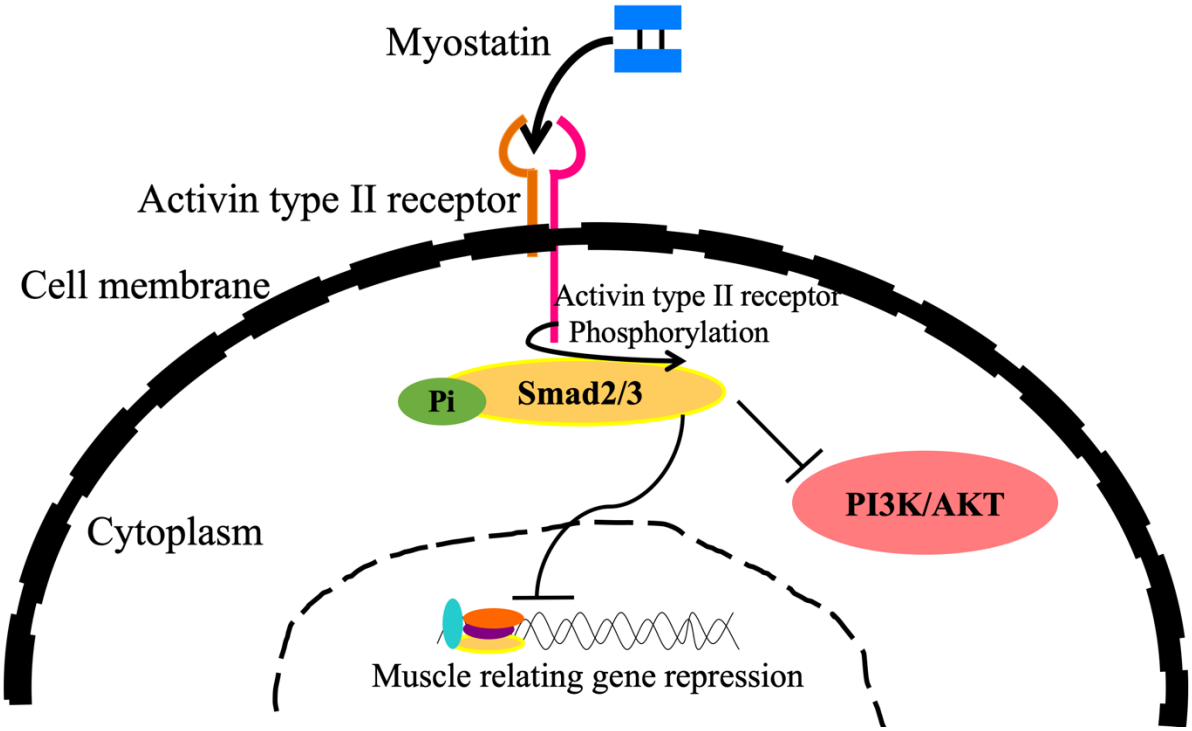

Figure 2. The signal transduction pathway of myostatin

Table 1. Homology matrix of myostatin amino acid sequences in 13 species (Shen, 2010)

Human (*Homo sepiens*_NP_005250.1)	100%												
Chimpanzee (*Pan troglodytes*_NP_001073388.1)	99.7%	100%											
Monkey (*Macaca mulatta*_NP_001073588.1)	99.7%	100%	100%										
Pig (*Sus scrofa*_O18831.1)	98%	98%	98%	100%									
Dog (*Canis lupus*_NP_001002959.1)	96%	96%	96%	97%	100%								
Cattle (*Bos taurus*_NP_001001525.1)	94%	94%	94%	96%	93%	100%							
Sheep (*Ovis aries*_O18830.1)	94%	94%	94%	93%	93%	93%	100%						
Goat (*Capra hircus*_Q6T5B8.2)	94%	94%	94%	95%	93%	93%	100%	100%					
Mouse (*Mus musculus*_NP_034964.1)	96%	97%	97%	96%	94%	93%	92%	92%	100%				
Rat (*Rattus norvegicus*_NP_034964.1)	95%	95%	95%	95%	93%	91%	91%	91%	98%	100%			
Chicken (*Gallus gallus*_NP_001001461.1)	92%	92%	92%	91%	90%	88%	88%	88%	91%	90%	100%		
Goose (*Anser anser*_ AAL35276.1)	91%	91%	91%	90%	89%	87%	87%	87%	90%	89%	97%	100%	
Duck (*Anas platyrhynchos*_Q8UWE0.1)	92%	92%	92%	91%	90%	88%	88%	88%	91%	90%	98%	98%	100%

Regulation of myostatin gene expression

To regulate the level of specific gene expression, there are various methods. Some strategies are demonstrated the regulation of myostatin gene expression. 5' regulatory region single nucleotide polymorphism (SNP), and SNP in myostatin gene affected myostatin gene expression. In addition, the amount of active protein, antagonist and antibody of myostatin are also can be used to regulate the myostatin activity.

SNP analysis of myostatin gene showed that myostatin 435GG/447AA genotype in both Duroc x Landrace (DL) and Duroc x Yorkshire x Landrace (DYL) pigs had significantly lower lean weight, lean percentage, anterior-end meat and posterior-end meat, while they had significantly thicker backfat either measured by ultrasound or carcass measurement (Jiang *et al*., 2002; Tu *et al*., 2013). The haploptype-1 (A435-A447-A879) of myostatin promoter up-regulated two-fold of the reporter gene expression in cell culture system (Bongiorni *et al*., 2014). The result from Liu and coworkers (Liu *et al*., 2010) results showed that G/A435-A/A447-T/A879 genotype resulted in significantly higher body weight on Day 21 (BW21), and significantly lower average daily weight gain from Day 21 to Day 70 (ADG2) in Duroc pigs (Liu *et al*., 2010). The result from Shen (2010) showed 5' regulatory region was highly conserved in bird and in mammal (Figure 3).

The inhibitor of myostatin or myostatin receptor antibody can be considered for therapy of skeletal muscle dystrophy or atrophy. Injection of myostatin antigen in mice induced production of maternal myostatin antibody. The offspring, both male and female, contained higher crude protein and lower crude fat compared with control group (Liang *et al*., 2007). Moreover, the JA16 Ab (myostatin monoclonal antibody)-treated mice gained approximately 10%

weight than the control and untreated mice (Whittemore *et al*., 2003). In mdx mouse, model of Duchenne muscular dystrophy (DMD), the decreased serum creatine kinase activity and increased extensor digitorum longus (EDL) mass were found in myostatin antibody-treated group (Bogdanovich *et al*., 2002). In addition, the antibody specifically against myostatin receptor, activin type II receptor (ActR II), increased the animal muscle growth. The interaction of ActR II and its antibody prevented myostatin from binding to ActR II, and interrupted myostatin intracellular signal transduction pathway (Lach-Trifilieff *et al*., 2005). In poultry, the animals from direct injection of myostatin antibody into yolk had significantly heavier carcass, leg muscles and breast muscles than that in the control group (Kim *et al*., 2007).

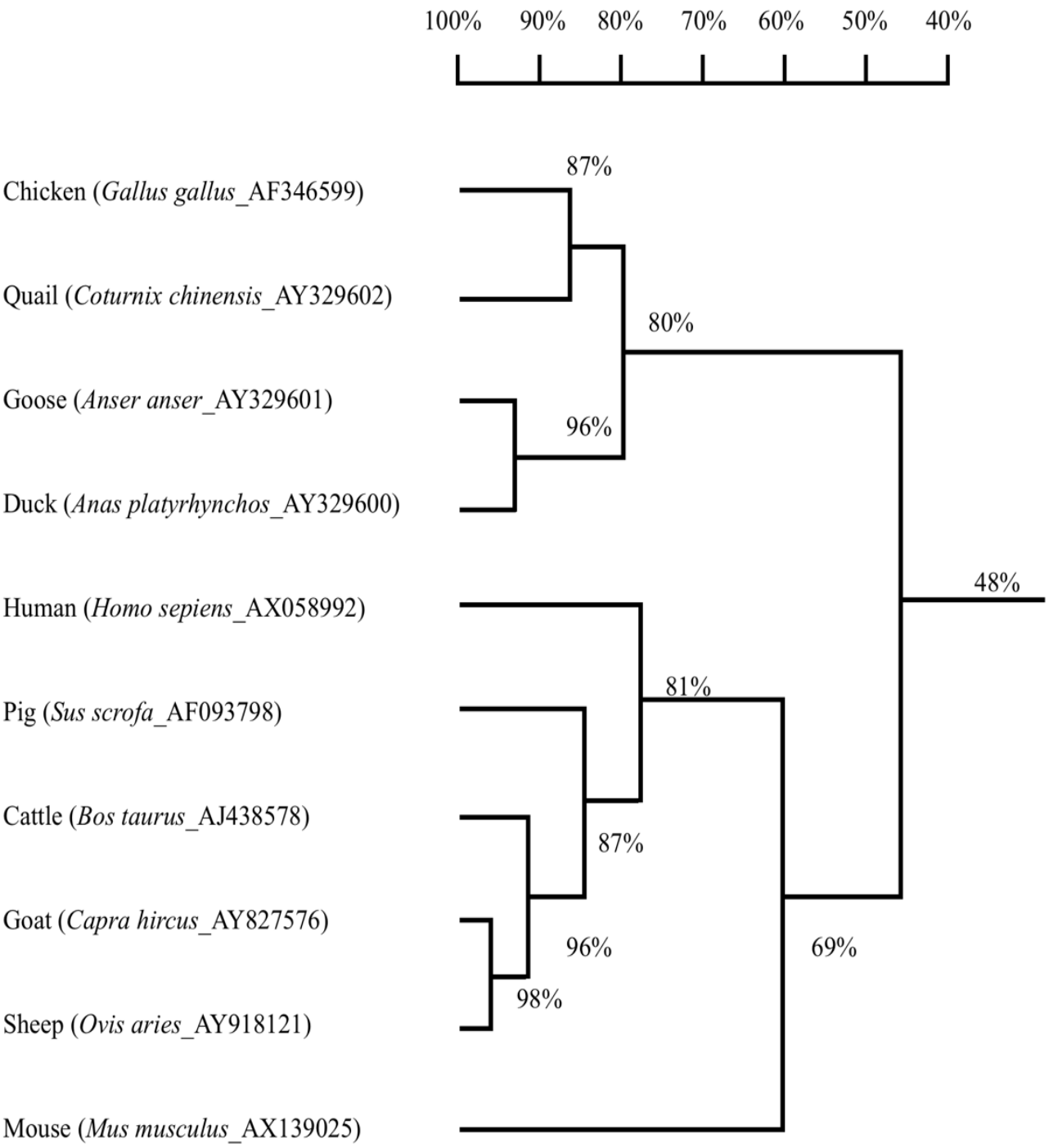

Figure 3. The 5' regulatory region sequence of myostatin homologous tree in 10 species (Shen, 2010)

Effect of myostatin on myoblast proliferation and differentiation

Myoblast fusion is a basic step within the muscle differentiation in most organisms. To achieve the complex of the system, the high expression level of *Pax* and *Mp20* are critical during myoblast fusion. In contrast to *Pax* and *Mp20*, low expression level of *mspo* increases myoblast fusion (Bataillé *et al*., 2010). Typically, these cells migrate long distance prior to fuse. In addition, the first fusion that occurs throughout embryogenesis, needs a smORF-encoding microprotein, Minion (microprotein inducer of fusion). Lacking Minion, myoblasts are still aligned but fail to form syncytial cell (Millay *et al*., 2013; Zhang *et al*., 2017). Myoblast fusion involves cell migration, adhesion and transduction. The regeneration and/or growth of muscle involves proliferation and differentiation of muscle satellite cells (Wei *et al*., 2015).

Myoblast proliferation

Myostatin affects the rate of myoblast proliferation by regulating cell cycle progression. In mouse myoblast C_2C_{12} cell culture, the overexpressing endogenous myostatin inhibited myoblast proliferation through cell-cycle arrest in the G1 and G2 phases. The cells prevent to transit to S phase where DNA synthesis occurs and M phase where cell division occurs, respectively (Dominique *et al*., 2006). The cell cycle arrest of G1 phase is mediated through up regulation of one of the cyclin-dependent kinase inhibitors, p21 (Manceau *et al*., 2008). In addition, myostatin also trend to reduce levels of cyclin dependent kinase-2 (Cdk2). The combination of the increased p21, and the decreased Cdk2 level resulted in a marked reduction of Cdk2 activity. Rb, a substrate of Cdk2, accumulated in an active hypophosphorylated state resulting in inhibition of cell cycle progression at G1 phase (Thomas *et al*., 2000). Rios and coworkers (Rios *et*

al., 2002) also reported an increase in the expression of p21 in the presence of ectopically overexpressed myostatin.

Myoblast differentiation

In mouse C_2C_{12} myoblasts, myostatin expression increases during differentiation (Rios *et al*., 2001). In addition, myostatin has also been shown to inhibit the myoblast differentiation of (Rios *et al*., 2002). To inhibit the myoblast differentiation, myostatin inhibit the expression of the MRFs, MyoD, myogenin Myf5 (Langley *et al*., 2002) as well as the late myogenic differentiation marker, myosin heavy chain (MHC) (Rios *et al*., 2002; Wei *et al*., 2015). Interestingly, the expression of p21, in contrast to proliferating myoblasts, is also down-regulated by myostatin during differentiation (Langley *et al*., 2002). The mechanism by which myostatin regulates MyoD has been partially elucidated. Langley and coworkers (Langley *et al*., 2002) showed that the presence of myostatin increased the phosphorylation of Smad 3, and increased the association of MyoD and Smad 3, which is known to repress MyoD activity (Liu *et al*., 2001). In addition, in embryo, myostatin signaling promotes the initiation of the terminal differentiation by activating MyoD expression in myoblasts (Manceau *et al*., 2008). It has also been shown that cells made quiescent by myostatin are not the same as reserve cells. During myoblast differentiation, a subset of myoblasts, termed reserve cells, remain quiescent and undifferentiated but retain the capacity to proliferate and differentiate. Reserve cells are characterized by a high expression of p130 and Myf5 and low MyoD expression. Myostatin-induced quiescent cells, however, do not express high protein level of p130 or Myf5 in myoblast differentiation, although they have decreased MyoD and MRF expression (Langley *et al*., 2002).

Characteristic of myostatin in muscle development

Deletion and inhibition of myostatin in animals lead mainly to increased muscle mass and reduced fat mass. In myostatin-null mice and double-muscled cattle breeds without myostatin present, there is an increase of muscle fiber number and hyperplasia of muscles cells were observed (Holmes and Ashmore, 1972; Gerrard and Judge, 1993; McPherron *et al*., 1996). Meanwhile, the results in mouse C_2C_{12} myoblasts had demonstrated that myostatin control muscle mass by inhibiting cell proliferation and protein synthesis. Myostatin shows negatively regulate satellite cell activation (Taylor *et al*., 2001; Zhang *et al.*, 2015). Forkhead box O (FoxO) is a key element of myostatin expression. The report showed that inhibition of the FoxO pathway increased in skeletal muscles during aged animal muscle atrophy (Reed *et al.*, 2012).

Licorice

Introduction of licorice

Glycyrrhiza uralensis, also known as licorice, has been used in food additive and medicinal herb in Asia for thousand years. It is perennial herb native from Mediterranean region, central to southern Russia and Turkey to Iran (Dastagir *et al*., 2016). Raw licorice roots mainly from the *Glycyrrhiza* species, such as *G. glabra*, *G. uralensis* and *G. inflata*, are usually used as medicinal material (Simmler *et al*., 2015). Licorice is multifunctional herb, and its special taste made it have been researched since 1940s. The pharmaceutical effect of licorice was first reported in 1950s and many scientists investigated licorice components analysis and its bioactivity in the same year. In 1950s, succus licorice was the major licorice used in daily life. Licorice was usually utilized for gastric ulcer therapy, but the effective molecule nor the medicinal mechanism was unknown. In traditional Chinese pharmacy, licorice was considered as drug to rejuvenate physical condition for fighting fatigue. In Egypt, Greece and Rome, licorices have been used since ancient times, and even now licorice is still used in the daily life (Dastagir *et al*., 2016).

Bioactivity of licorice

Most reports showed that licorices have anti-germ activity (Arifullah *et al*., 2013; Ren *et al*., 2015). One of the components in licorice, liquiritigenin, has estradiol (E_2) activity which can activate estrogen receptor-alpha and beta (ERα and ß) in MCF-7 and T47D breast cancer cells (Lecomte *et al*., 2017). Licorice has been used in hepatitis therapy for a long time. Chalcones, one of the licorice components, were relatively more active than other compounds for protecting liver (Kuang *et al*., 2017). The active compounds of licorice ethanol extract were increased to the PPAR-gamma ligand-binding activity which increased myoblast

and liver cell glucose sensitivity (Kuroda *et al*., 2010). Some components of licorice have ability to induce hepatic carcinoma apoptosis through ROS dependent pathway, such as LicA (Choi *et al*., 2014). In vivo study showed that glabridin in *G. glabra*, served as a dietary supplement, down regulated the sensitivity of oxidation in low-density lipoprotein (LDL), therefore, increased the possibility of the atherosclerotic lesion space (Fuhrman and Aviram, 2001; Grassi *et al*., 2010). These results may be associated with the absorption and binding of glabridin to the low-density lipoprotein and protection of the low-density lipoprotein from oxidization (Fuhrman *et al*., 1997; Messier *et al*., 2011).

The methanol extract of *G. glabra rhizomes*, at a dose of 150 mg/kg, has anti-arthritic activity in male rats mediated by inhibition of leukocyte migration, autoantigen production, and exhibition of anti-proteinase activity (Choudhary *et al*., 2015). Ahn and coworkers (2013) declared that *G. glabra* effectively inhibits the adipogenesis of 3T3-L1 cells. Glabridin has a therapeutic effect on metabolic disorders, such as diabetes and hyperglycemia, by modulating glucose metabolism through AMPK (AMP activated protein kinase) in skeletal muscle cells (Sawada *et al*., 2014). Yoshioka and coworkers (2018) demonstrated that licorice extract activates mTOR, p70S6K, and regulation of phosphorylation of FoxO3a. These factors were involved in protein synthesis, thus help to prevent type 2 diabetes mellitus-induced muscle atrophy.

Component Analysis of Licorice

Licorice contains many polar and nonpolar molecules. Licorice root contains chemical compounds such as triterpene saponins, flavonoids, coumarins, and other phenolics (Hosseinzadeh *et al*., 2015). In licorice, flavonoids contain diverse structures (Figure 4), which includes flavanones, chalcones, flavones, and

isoflavones (Zhang and Ye, 2009) (Table 2). Some of the active constituents of *Glycyrrhiza spp*. that belong to these flavonoid structures (Hosseinzadeh *et al*., 2015). Chalcones compose with open-chain flavonoid which has two aromatic rings connected by three-carbon α, ß unsaturated ketone (Figure 4) (Franceschelli *et al*., 2017). Mahapatra *et al.* (2015) showed that chalcones had efficiency effect on diabetes management and therapy.

Liquiritin, isoliquiritin and isoliquirigenin inhibit the growth of non-small cell lung cancer cells. The chemical constituents of licorice are extensively investigated by completely different authors (Hayashi *et al*., 2016; Siracusa *et al*., 2011). Although, few studies were dole out on the nutritious composition of *G. glabra.* Nutritionally, licorice may be a source of proteins, amino acids, polysaccharides and straight forward sugars, minerals (such as calcium, phosphorus, sodium, potassium, iron, magnesium, silicon, selenium, manganese, zinc, and copper), pectins, resins, starches, sterols, gums, oestrogens, tannins, phytosterols (sitosterol and stigmasterol), coumarins, vitamins (B1, B2, B3, B5, E, and C), and glycosides. An oversized variety of biological compounds have additionally been isolated, such as triterpenes, saponins (responsible for the sweet taste), and flavonoids (Rizzato *et al*., 2017; Wang *et al*., 2015). Recently, one of licorice main component, glabridin, was found to inhibit dexamethasone- induced protein degradation in C_2C_{12} myotubes and the muscle atrophy in mice. Glabridin reduced dexamethasone-induced expression of MuRF1 and Cbl-b through the inhibition of glucocorticoid receptor activation and acted as an antagonist (Yoshioka *et al*., 2019). Kinoshita *et al*. (2017) showed licorice flavonoid oil (LFO) in elderly diet significantly improved their body trunk muscle mass and body fat mass. Therefore, licorice may be used as the diet additives for improving animal muscle mass. In this thesis, the molecular screening system was established to screen the myostatin regulator in CMH, licorice was chosen to

investigate the effect of licorice ethanol extract on the proliferation and differentiation in L8 myoblasts.

Table 2. The flavonoid compounds in licorice

Structure	**Compounds**
Chalcones	isoliquiritigenin (Simmler *et al*., 2014) isoliquiritigenin apioside (Simmler *et al*., 2014) isoliquiritin (Simmler *et al*., 2014) neoisoliquiritin (Zhang and Ye, 2009) licochalcone A and B (Zhang and Ye, 2009)
Flavanones	liquiritigenin (Xu *et al*., 2013) liquiritin (Xu *et al*., 2013) liquiritin apioside (Xu *et al*., 2013)
Flavones (flavonols)	licoflavonol (Qiao *et al*., 2014; Zhang and Ye, 2009) isolicoflavonol (Qiao *et al*., 2014; Zhang and Ye, 2009)
Isoflavones	licoisoflavone (Zhang and Ye, 2009; Qiao *et al*., 2014) licoricone (Zhang and Ye, 2009; Qiao et al., 2014) gancaonin (Zhang and Ye, 2009; Qiao *et al*., 2014) angustone (Zhang and Ye, 2009; Qiao *et al*., 2014) isoangustone (Zhang and Ye, 2009; Qiao *et al*., 2014) glabrone (Zhang and Ye, 2009)
Isoflavans	glabridin (Zhang and Ye, 2009) hispaglabridin A and B (Zhang and Ye, 2009)

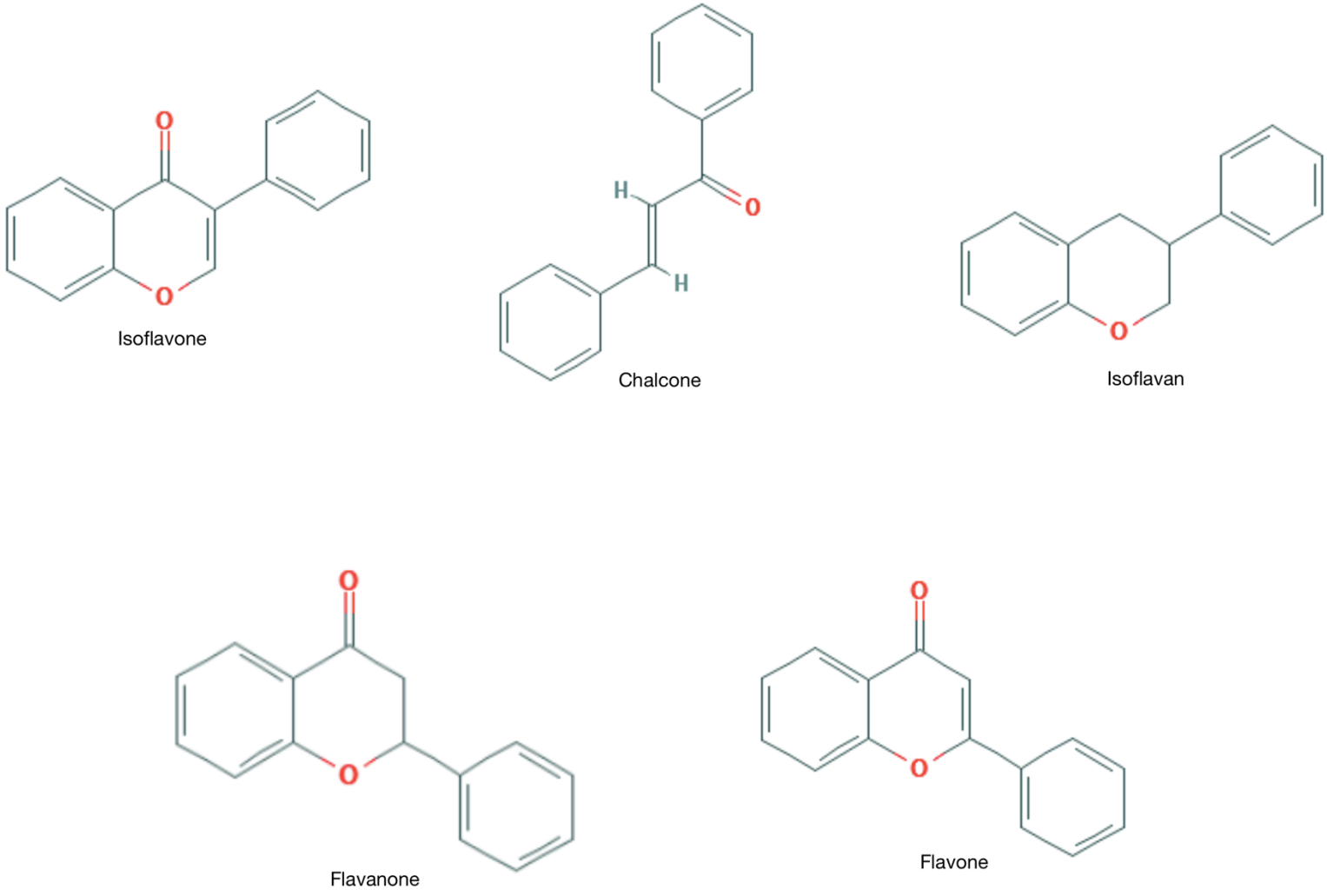

Figure 4. The chemical structures of major flavonoids in licorice.

MATERIALS AND METHODS

Plasmid construction

The primers for the construction of the plasmid were purchased from Mission Biotechnology. The primer sequences of mouse myostatin 5' regulatory region was designed according to *Mus musculas* AX139025. The primer sequences are listed below:

Forward mMSTN-PL-F-BglII-5': 5'-ATA AGA TCT CCT TTT TAA GTC CTA AGT CAC ACG G-3'

Reverse mMSTN-PL-R-BamHI-3': 5'-ATA GGA TCC CCA GGG AGT CCT GTA TAC TG-3'

Template DNA is isolated from C_2C_{12} myoblast. The PCR reaction mixture contains 500 ng genomic DNA, 0.4 μM forward primer, 0.4 μM reverse primer, 0.3 mM dNTPs, 4 μL 5X KAPA HiFi Fidelity Buffer, KAPA 0.5U HiFi HotStart DNA Polymerase (Kapa Biosystems, Roche, Basel, Switzerland). The reaction conditions are listed in Table 3. The restriction enzyme cutting site were added on the primers which use in PCR. After PCR, the product was purified by phenol chloroform extraction method. Restriction enzyme BglII 10 U/μL (A/GATCT) and BamHI (G/GATCC) with bovine serum albumin (BSA) 10 mg/mL (Promega, Madison, Wisconsin, United State). One μg pMetLuc2 reporter plasmid and 1 μg PCR product were digested with *Bgl*II and *BamH*I. And then, the 100 ng plasmid and 100ng PCR fragments were ligated by 0.5 U T4 DNA ligase (Promega, Madison, Wisconsin, United State) (Figure 1). The plasmid was confirmed by sequencing (Mission

Biotech, Taipei, Taiwan), and then the insert sequence was aligned with mouse 5' regulatory region sequence (*Mus musculas* AX139025).

Table 3. The PCR condition for amplification of mouse myostatin 5'-regulatory region

	Temperature (°C)	Time	Number of cycles
Denaturation	95°C	1 min	1
Denaturation	94°C	1 min	
Annealing	65°C	1 min	30
Extension	72°C	1 min	
Extension	72°C	5 min	1
	4°C	overnight	

Transfection of pMet Luc2 mMSTN into L8 cells

L8 cells were transfected with pMetLuc2 mMSTN by using Lipofectamine 2000 (Invitrogen, California, United States) accordance to manufacturer's recommendations.

L8 cells were cultured in DMEM with 10% FBS (Fetal bovine serum; Hyclone, GE Healthcare, Illinois, United States). Lipofectamine® reagent (9 μL) was diluted in 150 μL Opti-MEM® medium. Four μg plasmid DNA was added in 150 μL of Opti-MEM, and mixed gently and incubated for 5 minutes at room temperature. The diluted Lipofectamine 2000 and the diluted DNA were mixed and incubated for 30 minutes. DNA-Lipofectamine 2000 mixture (250 μL) was added into petri dish containing cells and medium, then mixed gently by rocking the dish back and forth. The cells were incubated 24 hrs. The medium was replaced by fresh medium containing 200 μg/mL G418. Consequently, the single cell colony is selected for future use.

Chinese medicinal herb extraction

Twenty seven CMHs were tested in this study. The CMHs were grinded to powder with grinder at 25000-30000 rpm. Herb powders (0.5 g) were added into 10 mL ethanol and stirred for10 hrs. The mixture was filtered with No.1 filter paper, and then put the mixture in hood to evaporate the alcohol. Gel-like product was collected and recorded the weight. The final product was dissolved in alcohol to final concentration of 40 mg/mL.

Chinese medical herb screening

The pMetLuc2 mMSTN transfected cells were cultured in DMEM with 10% FBS, and 1% Penicillin/streptomycin (10000 Unit/mL; Gibco). The L8 cells were plated in 96 well plate (Corning Inc., New York, United States). The final concentration of each well is 12000 cells/well. After the cells seeded for 24 h, cells were then treated with CMH ethanol extract. After 24 hrs treatment, the supernatant were collected for Luciferase activity assay. The cells were further performed MTT assay.

Protein extraction

The culture medium was removed and cells were washed three times with iced-cold PBS, pH 7.3. Then the cells were scraped with rubber policeman and collected in 500 μL homogenization solution [20 mM Tris (pH7.5), 0.25 mM Sucrose, 1 mM EGTA, 5 mM EDTA, 1 mM phenylmethane sulfonyl fluoride (PMSF), 25 μg/mL leupeptin, 50 mM 2-mercaptoethanol (2-Me), 1%NP-40]. After sonication, the lysate was centrifuged at 14000 xg for 20 min at 4℃. Cytosolic proteins were measured by the Bradford method using bovine serum albumin as standards (Bradford, 1976).

Western blot analysis

Lysate from the L8 myoblast was mixed with 6X sample buffer containing 62.5 mM Tris, 2% (w/v) sodium dodecyl sulfate, 10% (v/v) glycerol, 5% (v/v) 2-mercaptoethanol, and 0.0125% (w/v) bromophenol blue. The mixture was incubated at 100°C for 5 min and subjected to sodium dodecyl sulfate-polyacrylamide gel electrophoresis (SDS-PAGE). The separated proteins in the

gels were transferred onto the 0.45 μm polyvinylidene fluoride membrane. The membrane was incubated with a blocking solution consisting of 3% gelatin in TTBS (TBS with 0.05% tween20) for 1 hr at room temperature and hybridized with primary antibodies (myostatin 1:1000, GTX32624, GeneTex, California, United States; GAPDH 1:2000, MAB347, Chemicon, Burlington, Masschusettes, United States) for 1 hr at room temperature. And then, the membrane was incubated with horseradish peroxidase-conjugated secondary antibody for 1 hr at room temperature. Target bands were visualized using Bio-Rad Clarity Western ECL Substrate and detected by illuminance capturer (Vilber FUSION SL4 Spectra, France). The density of the specific band was determined using ImageJ image analysis software (National Institutes of Health, Bethesda, Maryland, United States).

Cell viability assay

MTT (5 mg/mL; 3-(4,5-dimethylthiazol-2-yl)-2,5-diphenyltetrazolium bromide), Sigma-Aldrich, St. Louis, Missouri, United States) was prepared in Phosphate Buffered Saline (PBS buffer, 137 mM NaCl, 2.7 mM KCl, 4.3 mM Na_2HPO_4, 1.47 mM KH_2PO_4; pH 7.4.) and filtered to sterilize and remove insoluble residue. Ten μL filtered MTT solution (yellow) was added to CMH treated cells in 96-well plate (Corning, New York, United States) and incubated at 37°C for 4 h. One hundred μL solubilization solution (10% SDS in 0.01M HCl) was added to each well and incubated for 24 hrs, and then used spectrostar nano microplate reader (BMG Labtech, Ortenberg, Germany) to read the plate with wavelength 595 nm (Denizot and Lang, 1986).

Luciferase assay

Luciferase substrate kit was obtained from Clonetech (TaKaRa, Japan). To prepare the 10x substrate stock solution, lyophilized secreted luciferase substrate was added substrate buffer, and then diluted the 10x substrate stock solution 1:10 in reaction buffer. Fifteen μL culture media from each sample was transferred into the 96-well plate, and then add 2.5 μL of 1x substrate to each sample. The luciferase activities were read by luminometer (Micrbeta TriLux, Perkin Elmer, Waltham, Massachusetts, United States) after mixing well.

HPLC (high performance liquid chromatography)

The dried root of *Glycyrrhiza uralensis Fisch* was obtained from a traditional pharmaceutical store in Taichung, Taiwan.

Alcohol dissolved samples were removed large particles by centrifuging at 13000 rpm for 10 min before loading. The Reverse phase HPLC separation is accomplished by using an isocratic elution with flow rate of 4.0 mL/min. Column temperature was 30°C. The mobile phase consists of water with ethanol (5% to 100% ethanol in 30 min). The injection volume was 200 μL of each sample. The total run time was 50 minutes for each injection. Column 5C18 AR-II K54606 (10 mm x 250 mm) (Cosmosil, Nacalai Tesque Inc., Japan) was used to separate the licorice crude extract and licorice fraction 3 (G3). Column 5C18 AR-II K54524 (4.6 mm x 250 mm) (Cosmosil, Nacalai Tesque Inc., Japan) was used to separate licorice fraction 3-3 (G3-3).

Statistical analysis

All experiments were carried out three to five times in triplicates. SAS was utilized to analyze data. In western blot and luciferase quantification, the data

were analyzed by proc ANOVA post-hoc Tukey's Honest Significant Difference test (P<0.05). The others were analyzed by proc GLM post-hoc Dunnett's test (P<0.05).

RESULTS

Construction of pMetLuc2mMSTNPL

Mouse myostatin 5'-regulatory region was amplified PCR and then inserted into pMetLuc2 plasmid (Figure 6). The myostatin 5'-regulatory region was confirmed by sequencing. The result showed the sequence was identical to the sequence in GenBank (mus musculas, AX139025) (Figure 5). The plasmid is referred to pMetLuc2mMSTNPL. The expression of reporter gene, luciferase, in this plasmid is under the control of myostatin 5'-regulatory region.

Screening CMH for inhibition of luciferase activity by molecular biological screening platform

Plasmid pMetLuc2mMSTNPL was used to transfect L8 myoblasts. After G418 selection, the morphology of transfected cell did not change when compare to the origin cells. The transfected L8 cells were used to screen the CMH for the inhibition of luciferase activity. Total 27 CMH were used to screen for the inhibition of luciferase activity (Figure 7). Amount 27 CMHs, licorice, perilla, houttuynia cordata, and jiaogulan inhibited the activity of luciferase in transfected cells. In addition, the inhibition of luciferase activity is negative correlated with cell growth. Licorice ethanol extract decreased luciferase activity at 200 μg/mL and 400 μg/mL in transfected L8 cells. In the meantime, it increased L8 cell growth (Figure 8A). However, high concentration of licorice ethanol extract showed cytotoxicity in transfected cells. The perilla ethanol extract showed similar effect on the inhibition of luciferase activity and cell growth (Figure 8B). Perilla extract decreased luciferase activity at 2000 μg/mL and 4000 μg/mL and increase cell growth at 500 μg/mL, 1000 μg/mL and 2000 μg/mL. *Houttuynia cordata*

ethanol extract increased transfected L8 cell growth at 1000 μg/mL, 2000 μg/mL and 4000 μg/mL, and it decreased luciferase activity at 4000 μg/mL and 8000 μg/mL (Figure 9A). Jiaogulan ethanol extract increased L8 cell growth at 2000 μg/mL and 4000 μg/mL, and it decreased luciferase activity at 2000 μg/mL and 4000 μg/mL (Figure 9B).

Positive correlation of luciferase activity with myostatin expression level in transfected L8 cells

To confirm myostatin protein quantity is positively correlated with luciferase activity in transfected L8 cells, Western blot analysis was performed. The transfected L8 cells were treated with licorice extract A (20 μg/mL) and B (10 μg/mL) for 24 h. The results showed that licorice A significantly decreased myostatin protein level (p<0.01) (Figure10). In addition, the luciferase activity was inhibited by Licorice A (Figure11). The results demonstrate that the luciferase activity is positive correlated with myostatin protein level. It indicated that the luciferase expression through the pMetLuc2mMSTNPL plasmid in L8 cell can be the indicator of the myostatin protein level.

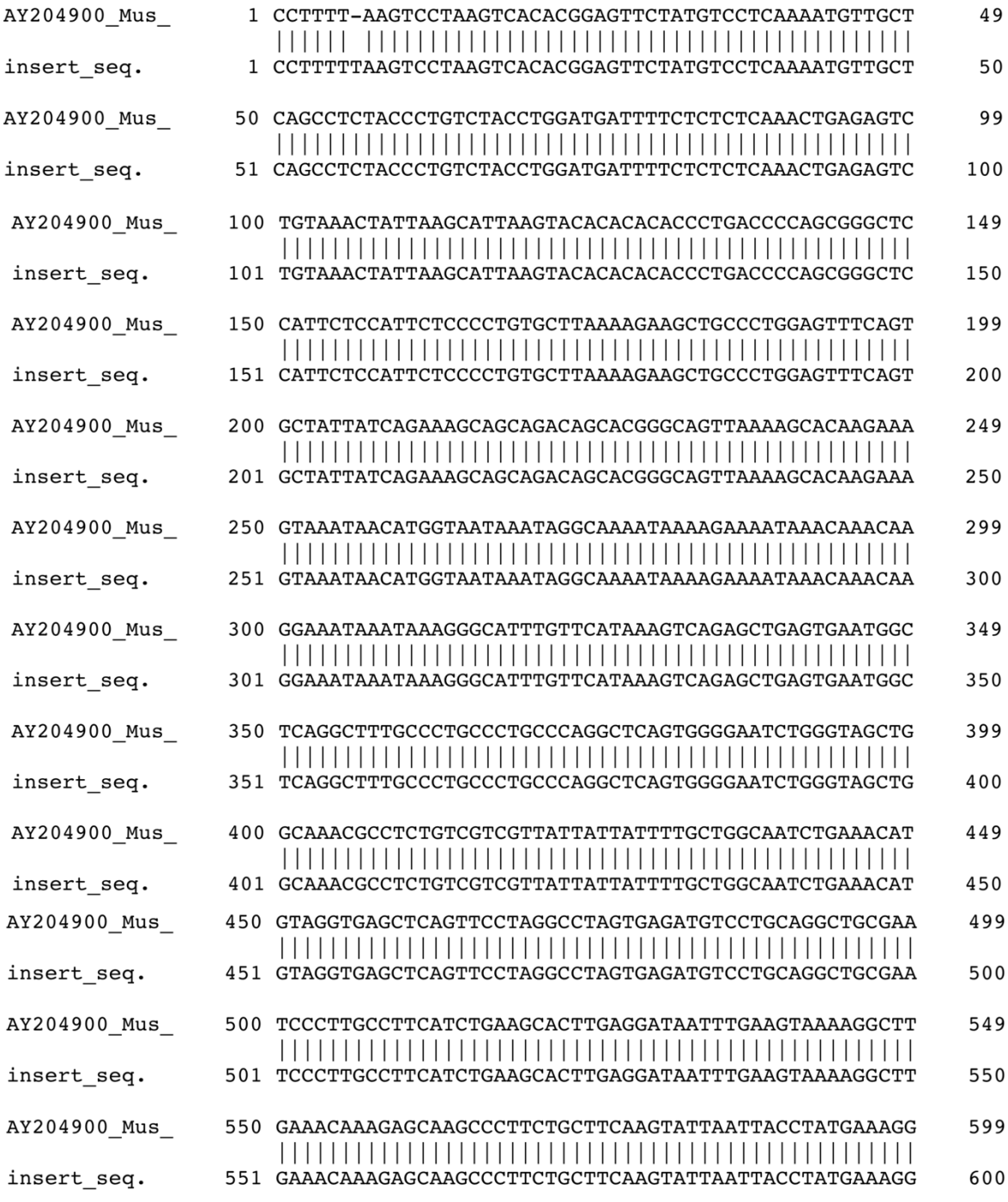

Figure 5. (continued)

```
AY204900_Mus_    600 GACTACATTTAGCTACTTATATTGCTAAATTATATGCCTCAAACCCCTTT    649
                     |||||||||||||||||||||||||||||||||||||||||||||||||||
insert_seq.      601 GACTACATTTAGCTACTTATATTGCTAAATTATATGCCTCAAACCCCTTT    650

AY204900_Mus_    650 AGTTGAGAAACTAAAGATAAGAGAAGCTAAGTACTGTGCCGTCTTTGTCA    699
                     |||||||||||||||||||||||||||||||||||||||||||||||||||
insert_seq.      651 AGTTGAGAAACTAAAGATAAGAGAAGCTAAGTACTGTGCCGTCTTTGTCA    700

AY204900_Mus_    700 TCGACTTAGAAGAGGCAAAATTGAGATTTGAACTCAGGTTTATTTGACTC    749
                     |||||||||||||||||||||||||||||||||||||||||||||||||||
insert_seq.      701 TCGACTTAGAAGAGGCAAAATTGAGATTTGAACTCAGGTTTATTTGACTC    750

AY204900_Mus_    750 TTCAGTCTCAGCTCACAATGGCAGTACAGTCTAAAAAAAAAAAAAAATCAC    799
                     |||||||||||||||||||||||||||||||||||||||||||||||||||
insert_seq.      751 TTCAGTCTCAGCTCACAATGGCAGTACAGTCTAAAAAAAAAAAAAAATCAC    800

AY204900_Mus_    800 AGGATCAATTTCCTCTGAGGTATATAGCAGCATGTGTAATGATAATTATG    849
                     |||||||||||||||||||||||||||||||||||||||||||||||||||
insert_seq.      801 AGGATCAATTTCCTCTGAGGTATATAGCAGCATGTGTAATGATAATTATG    850

AY204900_Mus_    850 ACATCGAAAAGAATTCTATGCAGAAAAATGAATTTTCCAGACAAATCTGA    899
                     |||||||||||||||||||||||||||||||||||||||||||||||||||
insert_seq.      851 ACATCGAAAAGAATTCTATGCAGAAAAATGAATTTTCCAGACAAATCTGA    900

AY204900_Mus_    900 CTTTATAGGCCTGCTCTAATATTGTCTTGTATAAAGAGGGCCAGATCACC    949
                     |||||||||||||||||||||||||||||||||||||||||||||||||||
insert_seq.      901 CTTTATAGGCCTGCTCTAATATTGTCTTGTATAAAGAGGGCCAGATCACC    950

AY204900_Mus_    950 TCAGGGTGTCTGCTTTGTGTCTGGTTTTCCTTCATCTTTAATGGTGGGCA    999
                     |||||||||||||||||||||||||||||||||||||||||||||||||||
insert_seq.      951 TCAGGGTGTCTGCTTTGTGTCTGGTTTTCCTTCATCTTTAATGGTGGGCA   1000

AY204900_Mus_   1000 AATCTAGTACATTATGGAAGCCCACTTTTTTTTTCCTCAAGAGATATAGA   1049
                     |||||||||||||||||||||||||||||||||||||||||||||||||||
insert_seq.     1001 AATCTAGTACATTATGGAAGCCCACTTTTTTTTTCCTCAAGAGATATAGA   1050

AY204900_Mus_   1050 TGCCTCTTAAAAATTTGATGAAAATGCATTAACTTTTCAAGCTACTGAGC   1099
                     |||||||||||||||||||||||||||||||||||||||||||||||||||
insert_seq.     1051 TGCCTCTTAAAAATTTGATGAAAATGCATTAACTTTTCAAGCTACTGAGC   1100

AY204900_Mus_   1100 TGCATTTTAGTTCACTGAGGCAGTAAATTGGGTGTATACTGTACAGGAAT   1149
                     |||||||||||||||||||||||||||||||||||||||||||||||||||
insert_seq.     1101 TGCATTTTAGTTCACTGAGGCAGTAAATTGGGTGTATACTGTACAGGAAT   1150

AY204900_Mus_   1150 GGTGGTGACCTAAAAATAAATATTTGATACAAGCCACCATAGTCTCTTGG   1199
                     |||||||||||||||||||||||||||||||||||||||||||||||||||
insert_seq.     1151 GGTGGTGACCTAAAAATAAATATTTGATACAAGCCACCATAGTCTCTTGG   1200

AY204900_Mus_   1200 GGTGTGTGTAAGGGGAGTAATGAATTAAAATTCTAAAGACTCCTCAGCTT   1249
                     |||||||||||||||||||||||||||||||||||||||||||||||||||
insert_seq.     1201 GGTGTGTGTAAGGGGAGTAATGAATTAAAATTCTAAAGACTCCTCAGCTT   1250
```

Figure 5. (continued)

```
AY204900_Mus_   1250 CCCAAACAGGAGGAGGAACTCTGTGGCCTGGAAGCGTCCTCTGTCCCTGC   1299
                     ||||||||||||||||||||||||||||||||||||||||||||||||||
insert_seq.     1251 CCCAAACAGGAGGAGGAACTCTGTGGCCTGGAAGCGTCCTCTGTCCCTGC   1300

AY204900_Mus_   1300 TGCTGTGTTTGTTCAGCTCTTTAAGAGTTCACCCCATTCGATCTTGTGGC   1349
                     ||||||||||||||||||||||||||||||||||||||||||||||||||
insert_seq.     1301 TGCTGTGTTTGTTCAGCTCTTTAAGAGTTCACCCCATTCGATCTTGTGGC   1350

AY204900_Mus_   1350 TCCTAAAGCCAAGGGTGAAAGTTTGATCCTTGCAGAGGCCACTTAAATTC   1399
                     ||||||||||||||||||||||||||||||||||||||||||||||||||
insert_seq.     1351 TCCTAAAGCCAAGGGTGAAAGTTTGATCCTTGCAGAGGCCACTTAAATTC   1400

AY204900_Mus_   1400 AGAGAACAAAAAGCACCATTCTCTGCCCTAGACTCTAGCCCAGATCCCTG   1449
                     ||||||||||||||||||||||||||||||||||||||||||||||||||
insert_seq.     1401 AGAGAACAAAAAGCACCATTCTCTGCCCTAGACTCTAGCCCAGATCCCTG   1450

AY204900_Mus_   1450 CCAGGTGTCTGCCCTCTGGTCAAAATGAGACGCTGGCAAAGGGGTGCTAG   1499
                     ||||||||||||||||||||||||||||||||||||||||||||||||||
insert_seq.     1451 CCAGGTGTCTGCCCTCTGGTCAAAATGAGACGCTGGCAAAGGGGTGCTAG   1500

AY204900_Mus_   1500 CCTGTGACAGTATGGGAACGCAACAAAGGACACCCCTCTACATGCGACTT   1549
                     ||||||||||||||||||||||||||||||||||||||||||||||||||
insert_seq.     1501 CCTGTGACAGTATGGGAACGCAACAAAGGACACCCCTCTACATGCGACTT   1550

AY204900_Mus_   1550 GCTCTTTGTGTGCTCACGGGACCTGACATCATTCACAGAGAACACAGATT   1599
                     ||||||||||||||||||||||||||||||||||||||||||||||||||
insert_seq.     1551 GCTCTTTGTGTGCTCACGGGACCTGACATCATTCACAGAGAACACAGATT   1600

AY204900_Mus_   1600 GCACTTTACTGTCAGCCCTGGAAGTCTGAGTCAAACTGAAATAATGCTCC   1649
                     ||||||||||||||||||||||||||||||||||||||||||||||||||
insert_seq.     1601 GCACTTTACTGTCAGCCCTGGAAGTCTGAGTCAAACTGAAATAATGCTCC   1650

AY204900_Mus_   1650 AGCGCTACTTACAAAAATCCATTATCTACTCGGCCTAAGTACAGAGCCTG   1699
                     ||||||||||||||||||||||||||||||||||||||||||||||||||
insert_seq.     1651 AGCGCTACTTACAAAAATCCATTATCTACTCGGCCTAAGTACAGAGCCTG   1700

AY204900_Mus_   1700 GCCTCCTCGCTGACAGGATTCTGTTGGCAATCAAAAAAAAAAAAAAAAAA   1749
                     ||||||||||||||||||||||||||||||||||||||||||||||||||
insert_seq.     1701 GCCTCCTCGCTGACAGGATTCTGTTGGCAATCAAAAAAAAAAAAAAAAAA   1750

AY204900_Mus_   1750 AAAAGCAACACTCAGTCTTTAGTCTGTATCTCTGTAATAGAAAATAGCAA   1799
                     ||||||||||||||||||||||||||||||||||||||||||||||||||
insert_seq.     1751 AAAAGCAACACTCAGTCTTTAGTCTGTATCTCTGTAATAGAAAATAGCAA   1800

AY204900_Mus_   1800 TACTTATAAGCTGAAATCAAGCACAGGTTTTATGTTAGTCAAAGCCATTA   1849
                     ||||||||||||||||||||||||||||||||||||||||||||||||||
insert_seq.     1801 TACTTATAAGCTGAAATCAAGCACAGGTTTTATGTTAGTCAAAGCCATTA   1850
```

Figure 5. (continued)

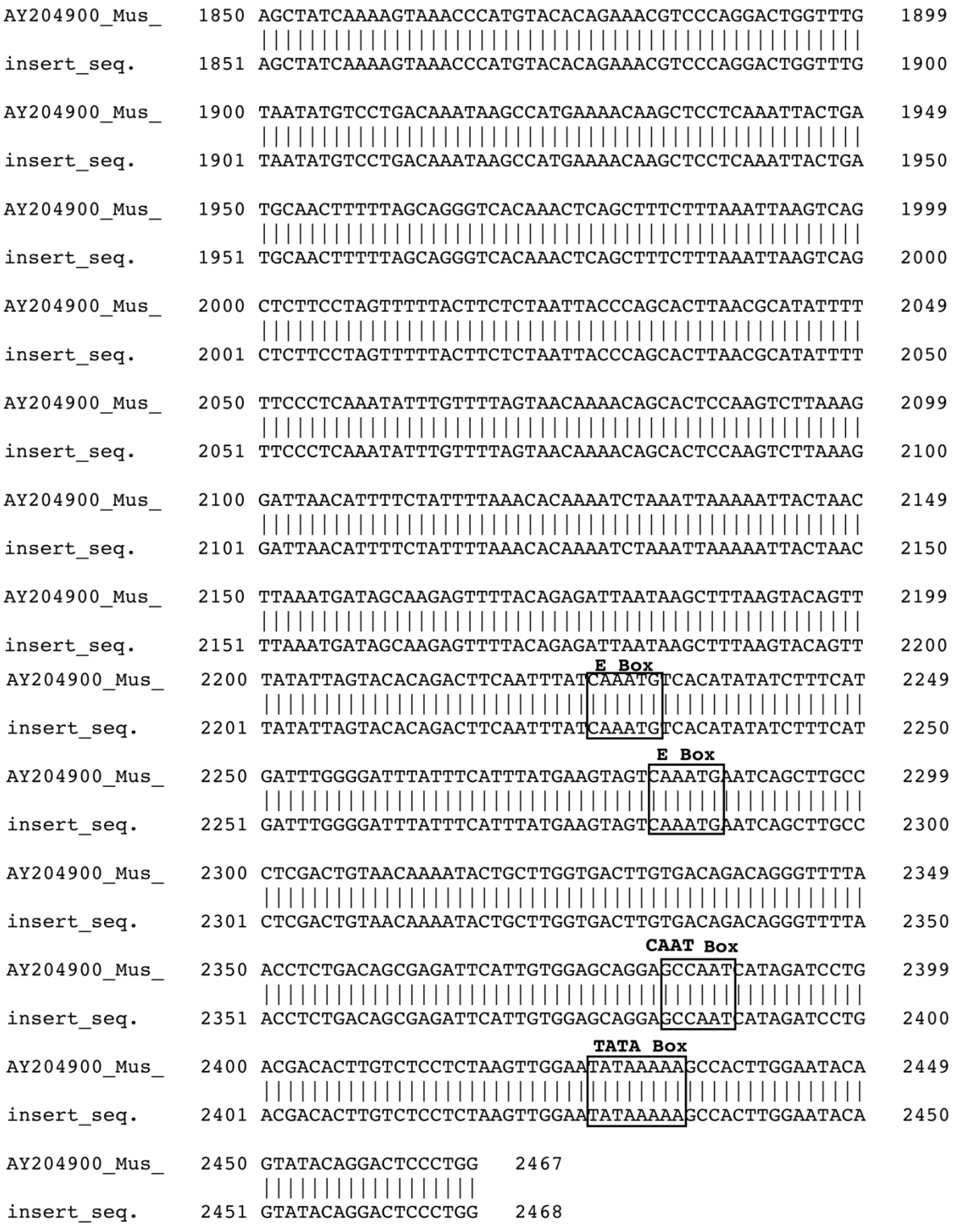

Figure 5. The sequence of plasmid insert aligned with NCBI Mouse myostatin 5'-regulatory region (*Mus musculas*, AX139025). Labeled the location of E-Box, CAAT Box and TATA Box.

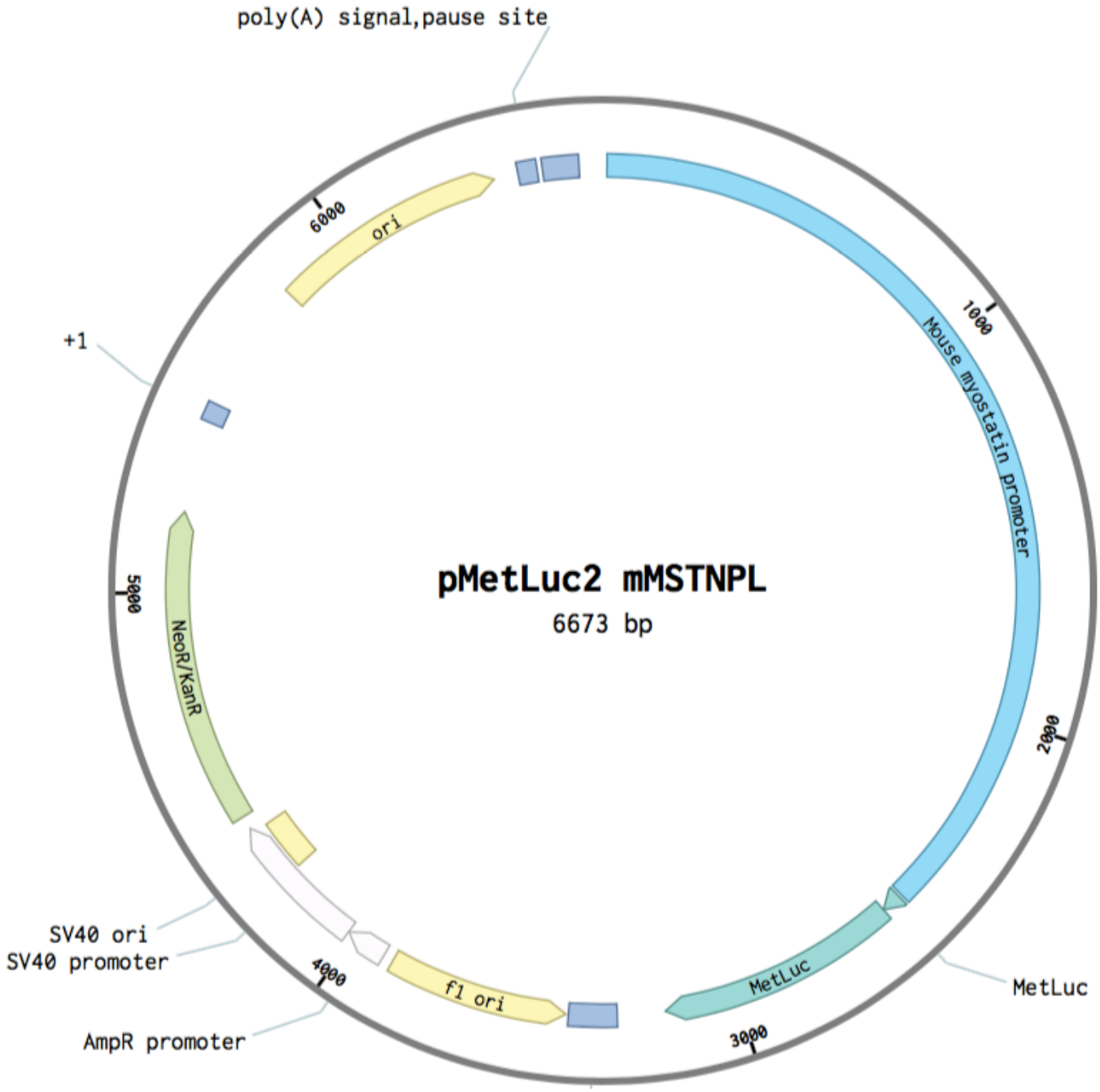

Figure 6. The plasmid map of pMetLuc2mMSTNPL. This plasmid was inserted a 2468 bp mouse myostatin 5'-regulatory region.

黃芩	白朮	甘草	艾葉	麥芽	杜仲	黃柏
Skullcap	Bai zhu	Licorice	Artemisia indica.	Malt	Eucommia ulmoides	Huang bai
小金英	牛蒡	黃耆	紫蘇	黨蔘	天麻	大蒜
Ixeris chinensis	greater burdock	Astragalus	Perilla	Codonopsis pilosula	Gastrodia elata	Allium sativum
玉竹	肉桂	麝香草	迷迭香	小茴香	肉豆蔻	秦皮
Solomon's Seal	Chinese cinnamon	Thyme	Rosemary	Fennel Bulbs	Nutmeg	Qinpi
洋香菜	魚腥草	陳皮	絞股藍	茯苓	川七	
Parsley	Houttuynia cordata	Chenpi	Jiaogulan	Wolfiporia extensa	Anredera cordifolia	

Figure 7. The Chinese name and common name of 27 CMHs. Black square: Herb showed inhibition of luciferase activity.

(A)

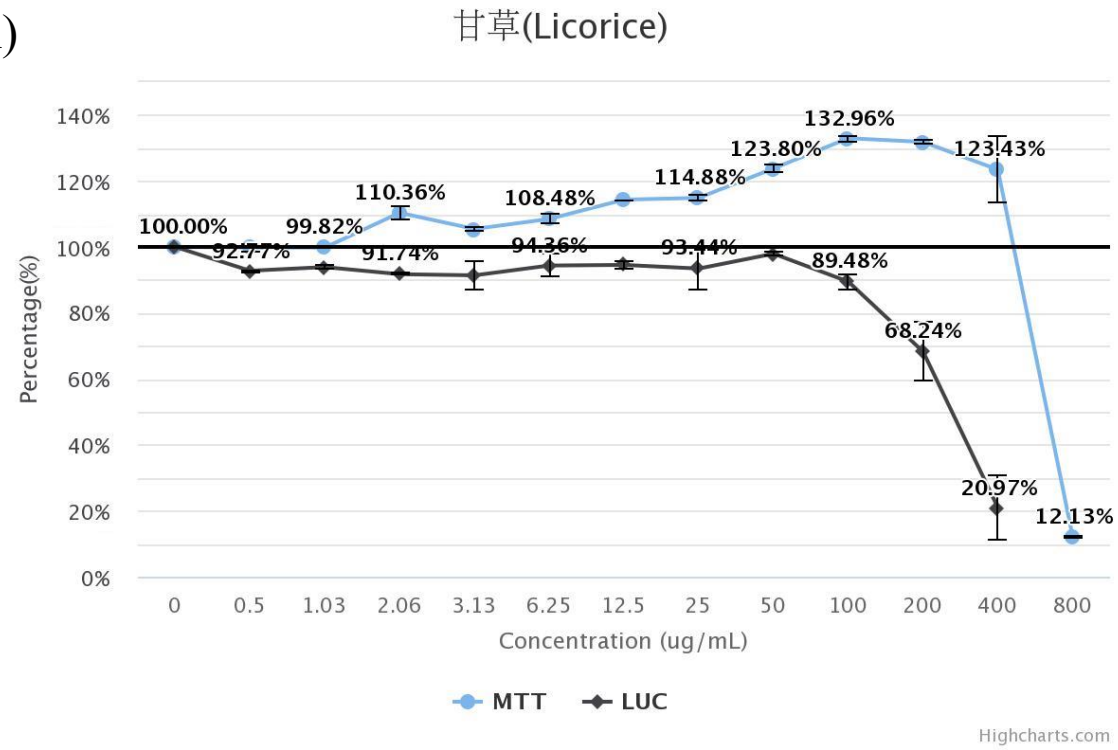

(B)

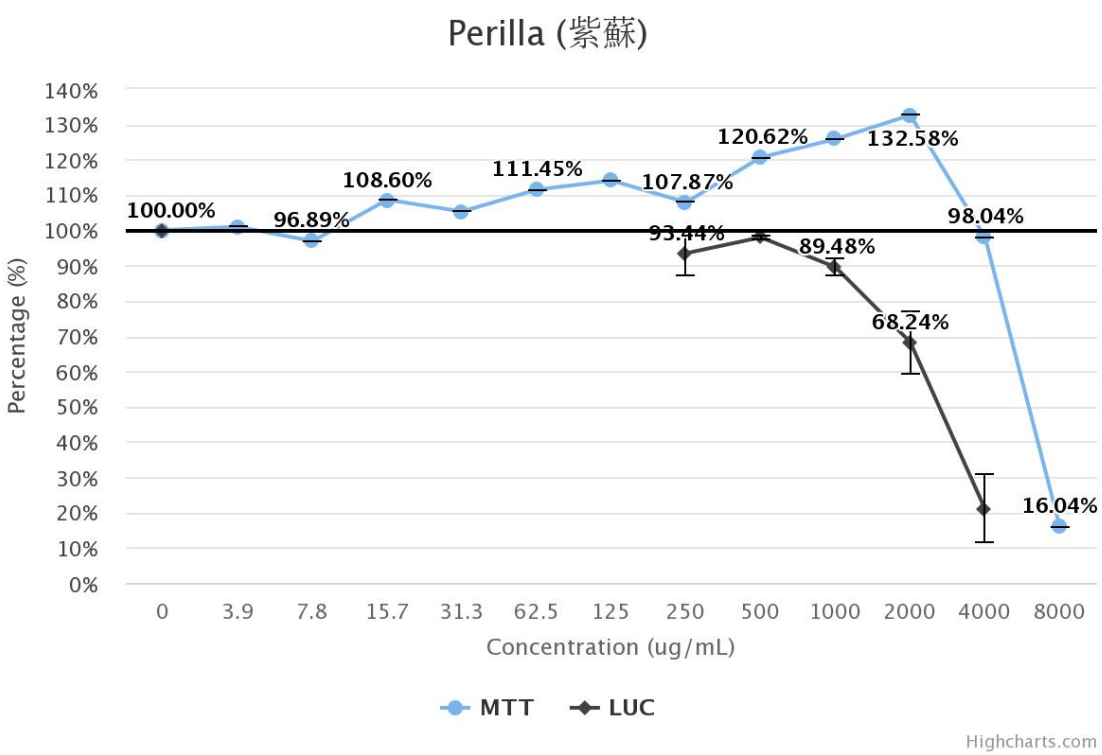

Figure 8. Effect of licorice ethanol extract (A) and perilla ethanol extract (B) on luciferase activity and cell growth in transfected L8 cells.

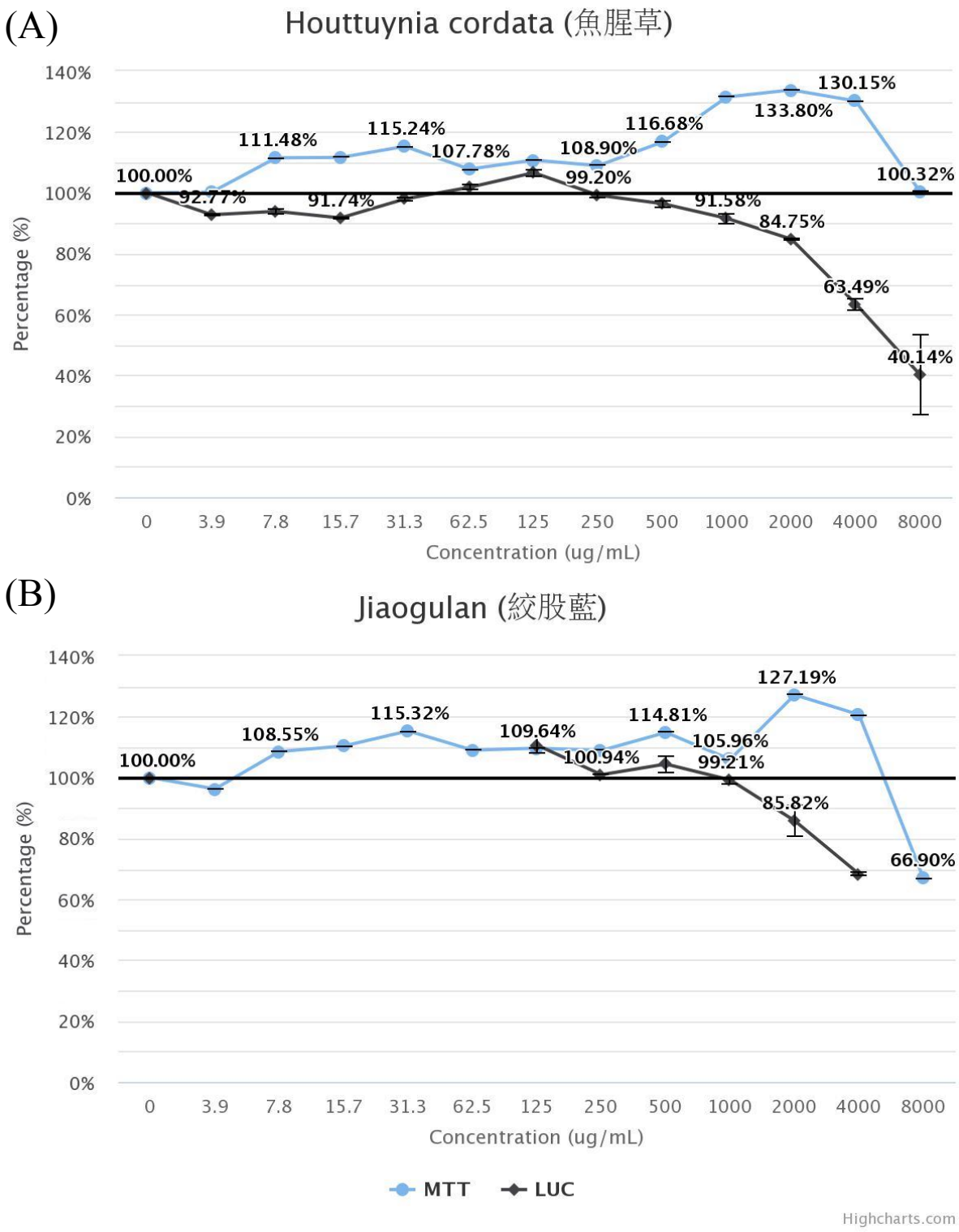

Figure 9. Effect of *Houttuynia cordata* ethanol extract (A) and jiaogulan ethanol extract (B) on luciferase activity and cell growth in transfected L8 cells.

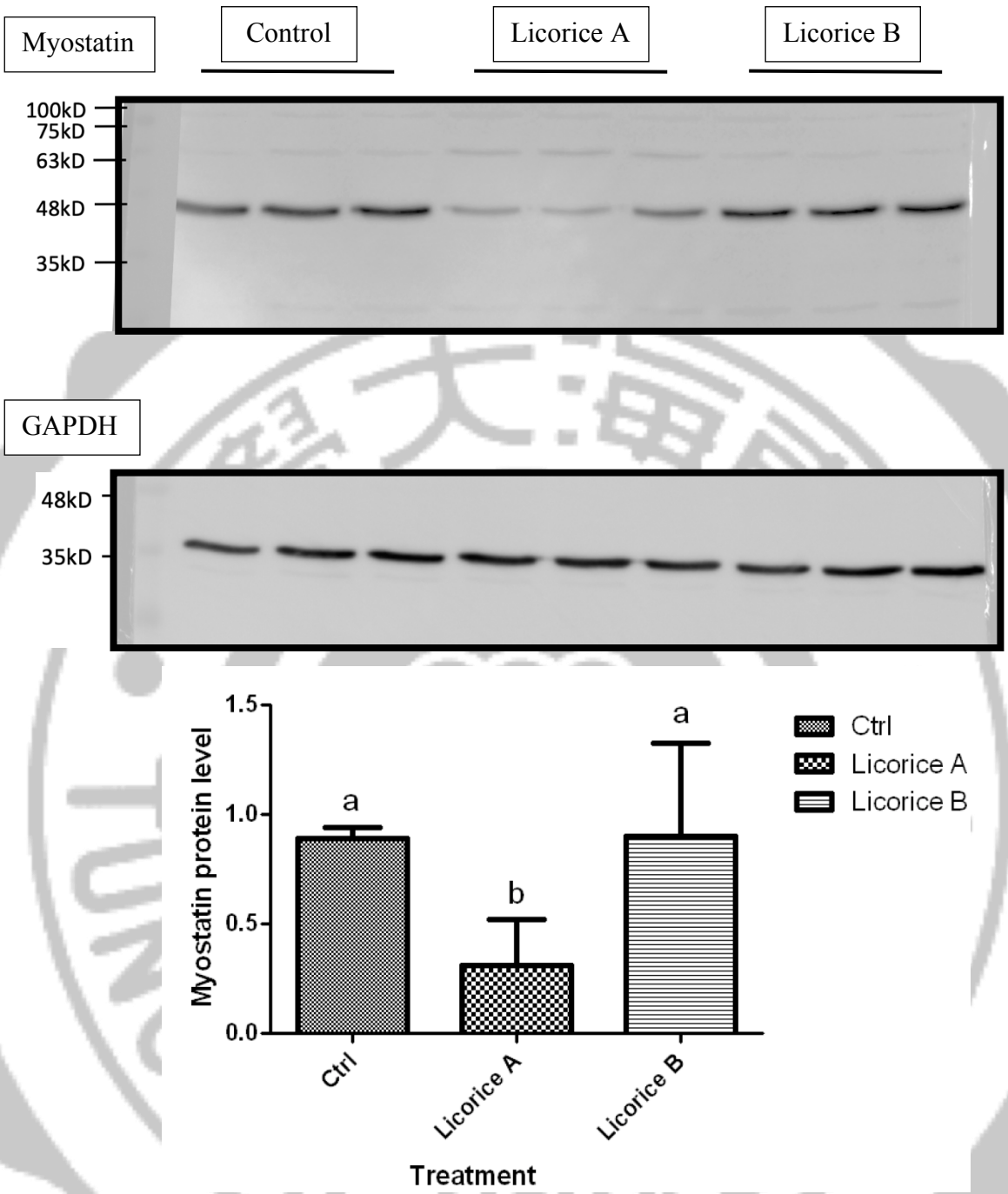

Figure 10. Effect of licorice ethanol extract on myostatin protein levels in transfected L8 cells. The cells were treated with different concentration of licorice ethanol extract (Licorice A: 20 μg/mL and Licorice B: 10 μg/mL), and GAPDH served as internal control.

(A)

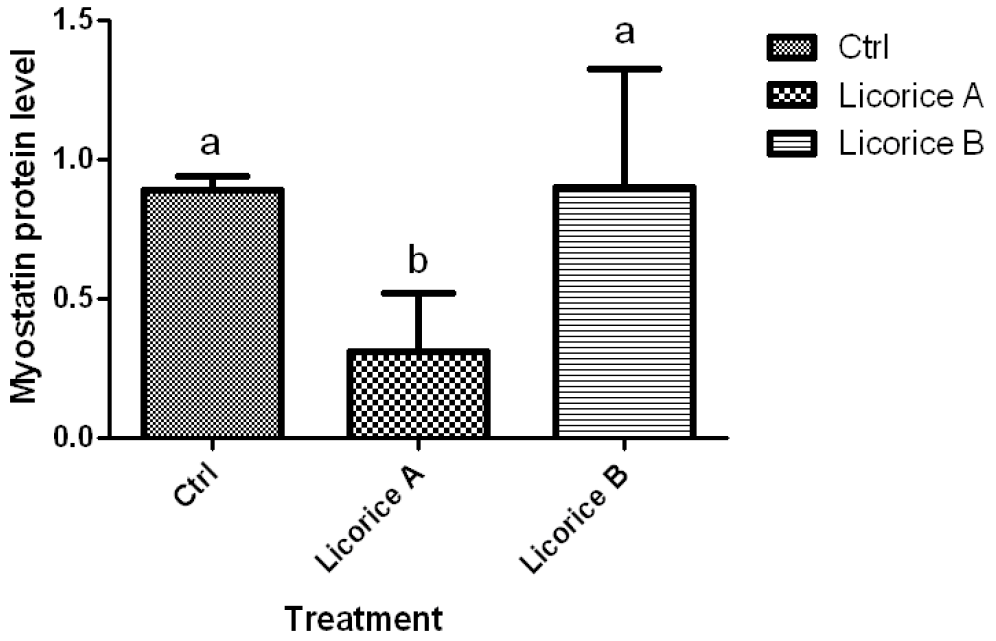

(B)

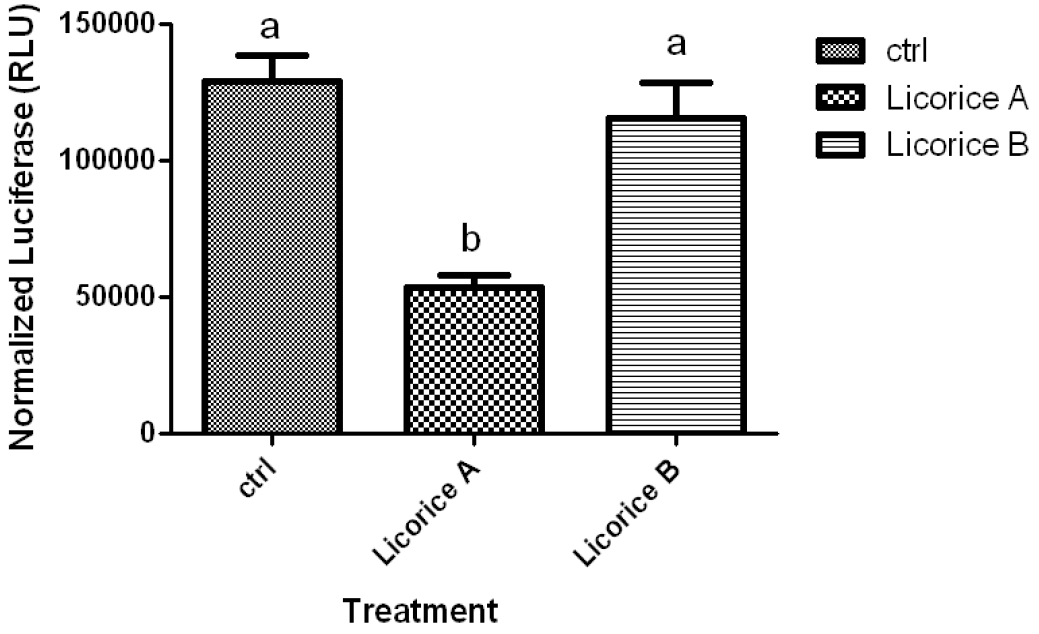

Figure 11. Effect of licorice ethanol extract on myostatin concentrations and luciferase activities. A: myostatin protein level from figure 10; B: luciferase activity

The isolation of active fraction from licorice ethanol extract by HPLC

To identify the active ingredient from licorice, high performance liquid chromatography (HPLC) was used. During the HPLC separation, 2.4 mL licorice ethanol extract was applied to polar solid phase and eluted in five fractions based on retention time, G1 (0-10 min), G2 (10-20 min), G3 (20-30 min), G4 (30-40 min), G5 (40-50 min) (Figure 12B). The ethanol gradient was from 5% to 100% in 30 min, and then 100% ethanol for another 15 min. The fractions were dried by vacuum centrifugation, then dissolved in ethanol (40 mg/mL). Each fraction was determined the inhibition of luciferase activity by the method described previously. Amount the 5 fractions, licorice fraction 3 (G3) significantly increased transfected L8 cell growth, and it decreased luciferase activity (Figure 13-15). Pure glabridin, which is the main compound of licorice ethanol extract, also applied to the screening platform. Glabridin increased L8 cell growth, in addition, luciferase activity was decreased by glabridin.

To identify the active ingredient in G3, G3 was further applied into polar solid phase and eluted in five fractions based on retention time, G3-1 (0-10 min), G3-2 (10-20 min), G3-3 (20-30 min), G3-4 (30-40 min), G3-5 (40-50 min) (Figure 16B.). The ethanol gradient for G3 was 45% for 5 min, 45% to 100% for 40 min, and then kept 100% for 5 min. The fractions were dried by vacuum centrifugation, then dissolved in ethanol (40 mg/mL). Each fraction was determined the inhibition of luciferase activity by the method described previously. Licorice fraction G3-2 and G3-3 increased transfected L8 cell growth, in the same time, they inhibited luciferase activity in transfected L8 cell (Figure 17). The glabridin was applied into the same column with the same elution condition. The result showed that the retention time for glabridin is before 20 min (Figure 16A). This result imply that glabridin may contribute the effect of G3-2

on cell growth and luciferase activity, while G3-3 contains other unknown component(s) affected the cell growth and luciferase activity.

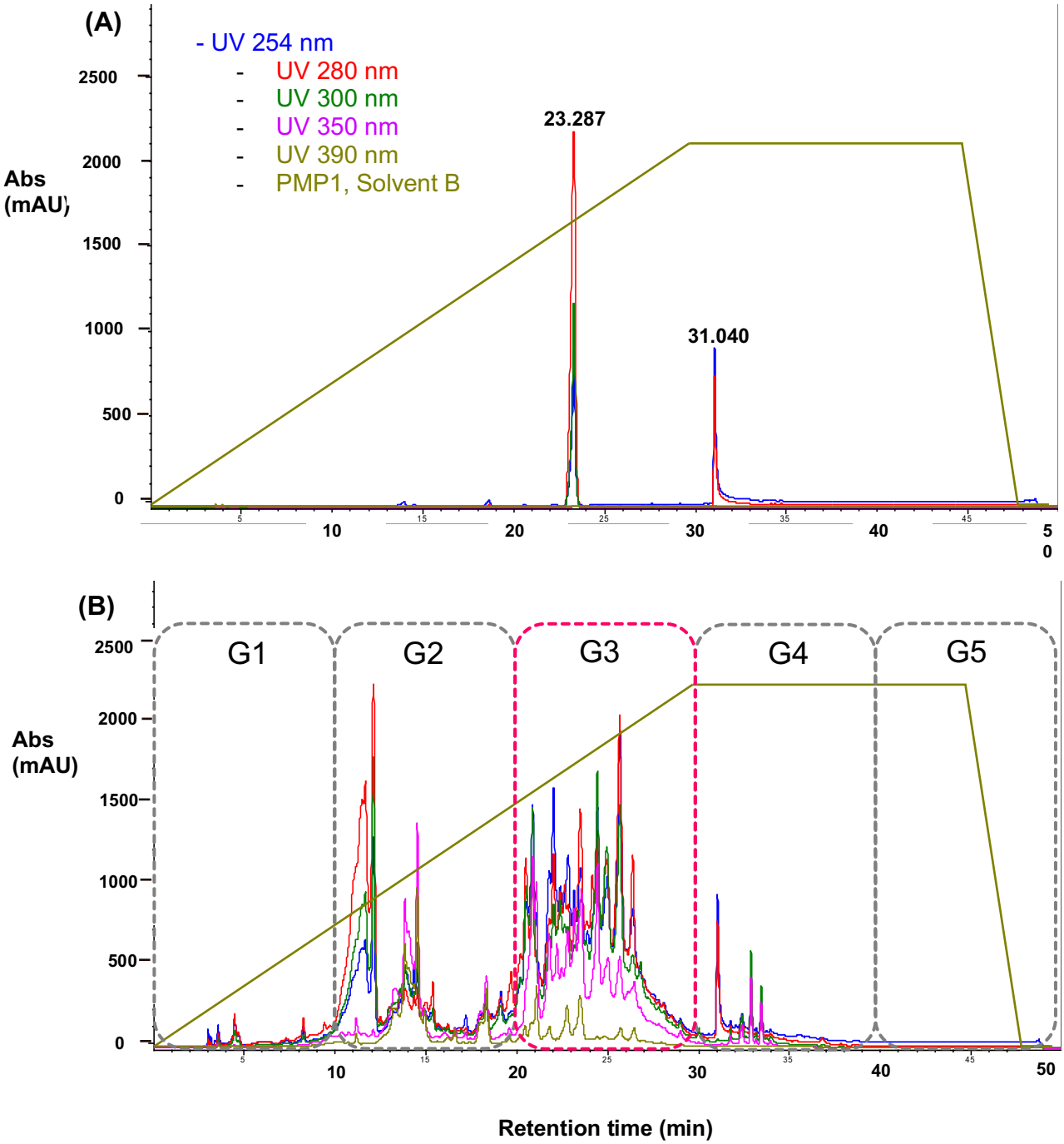

Figure 12. HPLC profile of glabridin (A) and licorice ethanol extract (B). The elution was separated in five fraction (10 min for each).

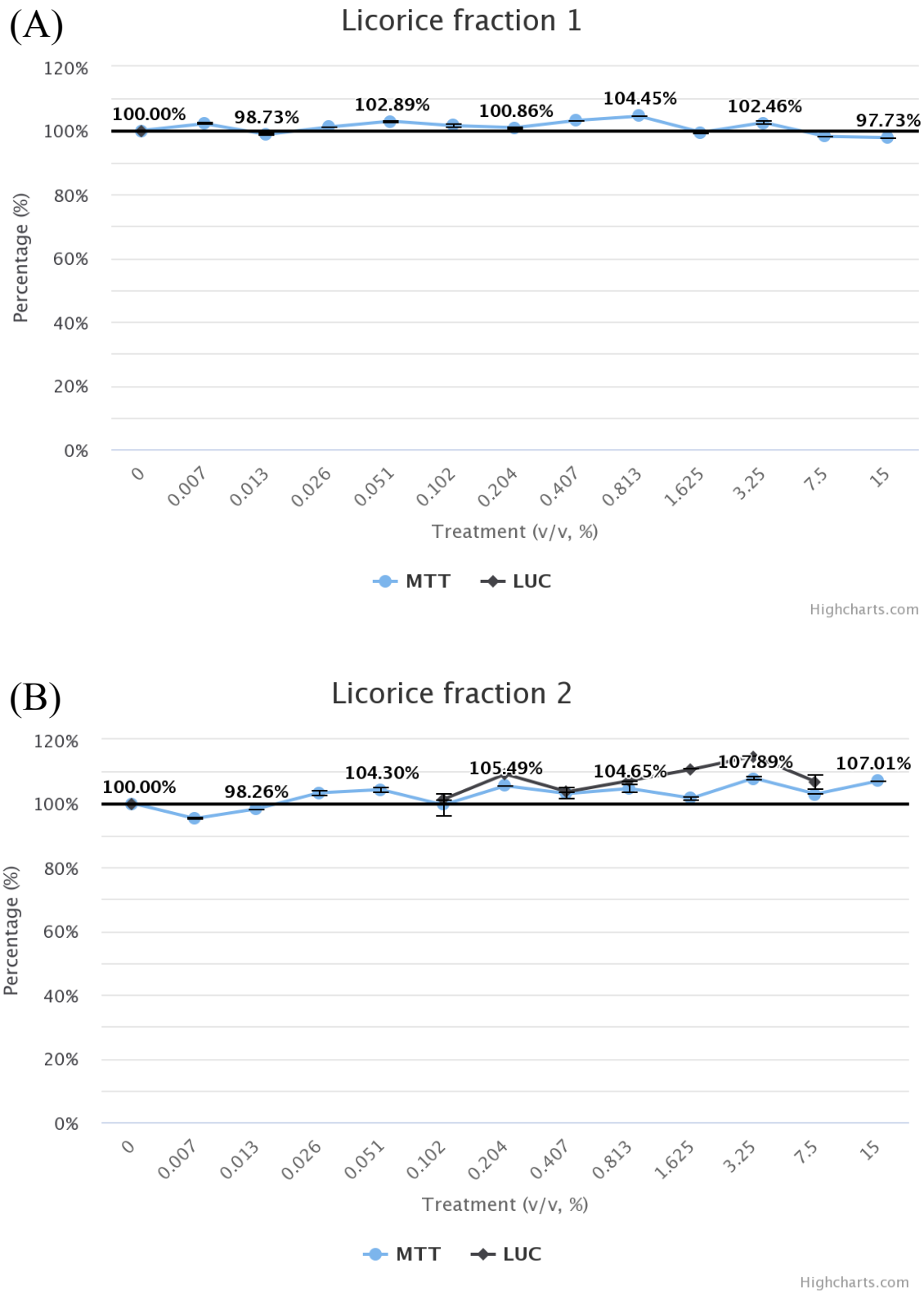

Figure 13. Effect of licorice fraction 1 and fraction 2 by HPLC on cell growth and luciferase activity in transfected L8 cells.

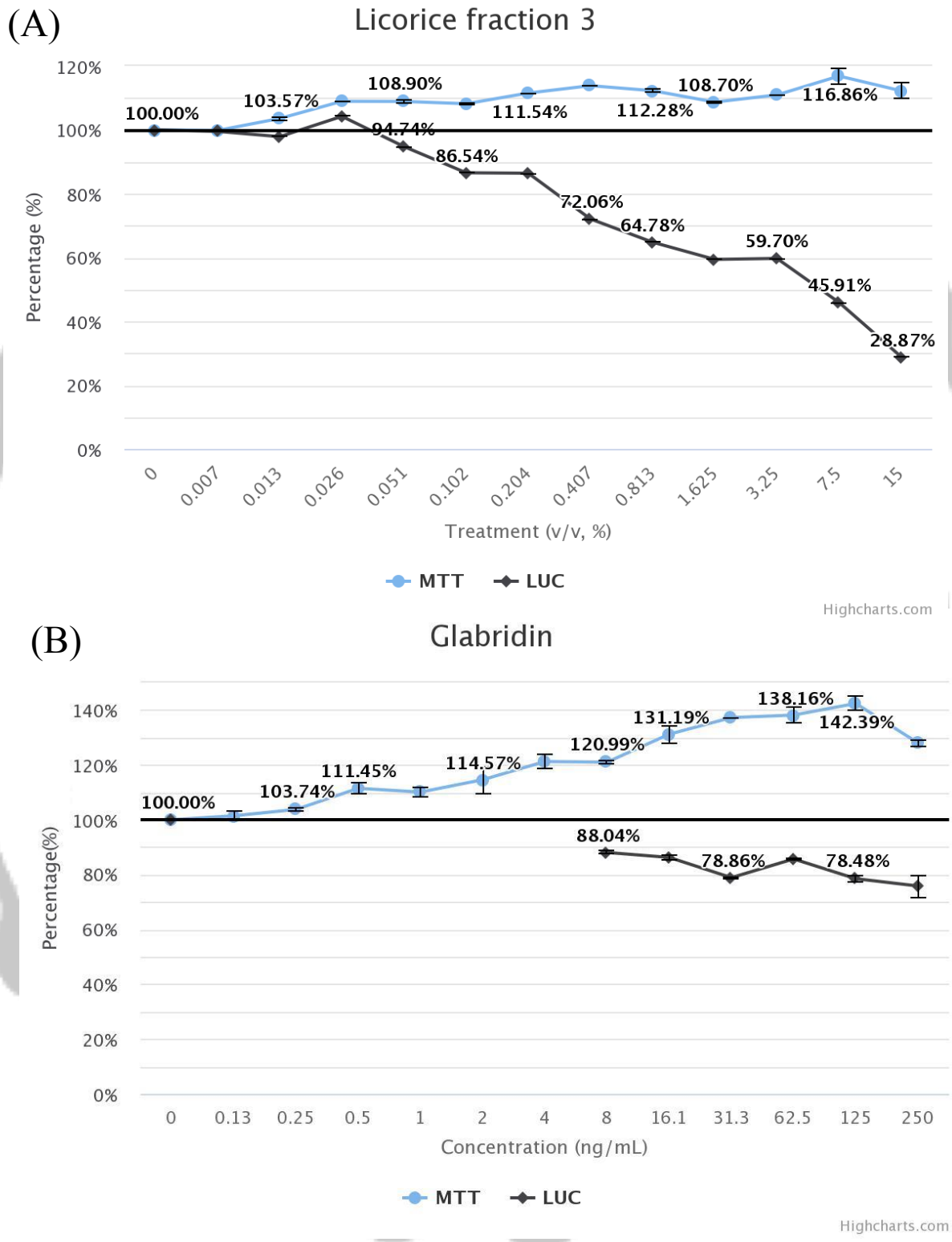

Figure 14. Effect of licorice fraction 3 and glabridin by HPLC on cell growth and luciferase activity in transfected L8 cells.

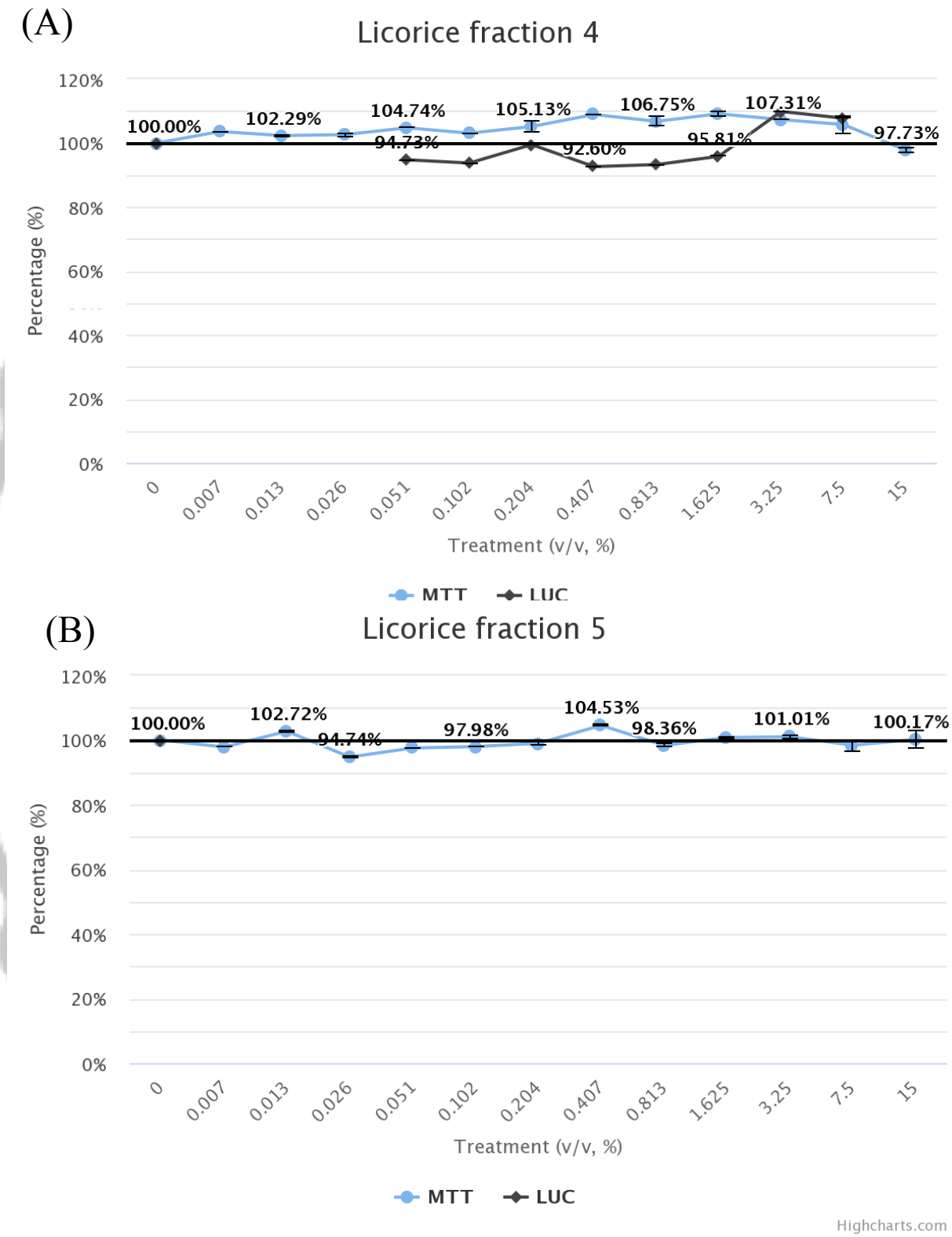

Figure 15. Effect of licorice fraction 4 and fraction 5 by HPLC on cell growth and luciferase activity in transfected L8 cells.

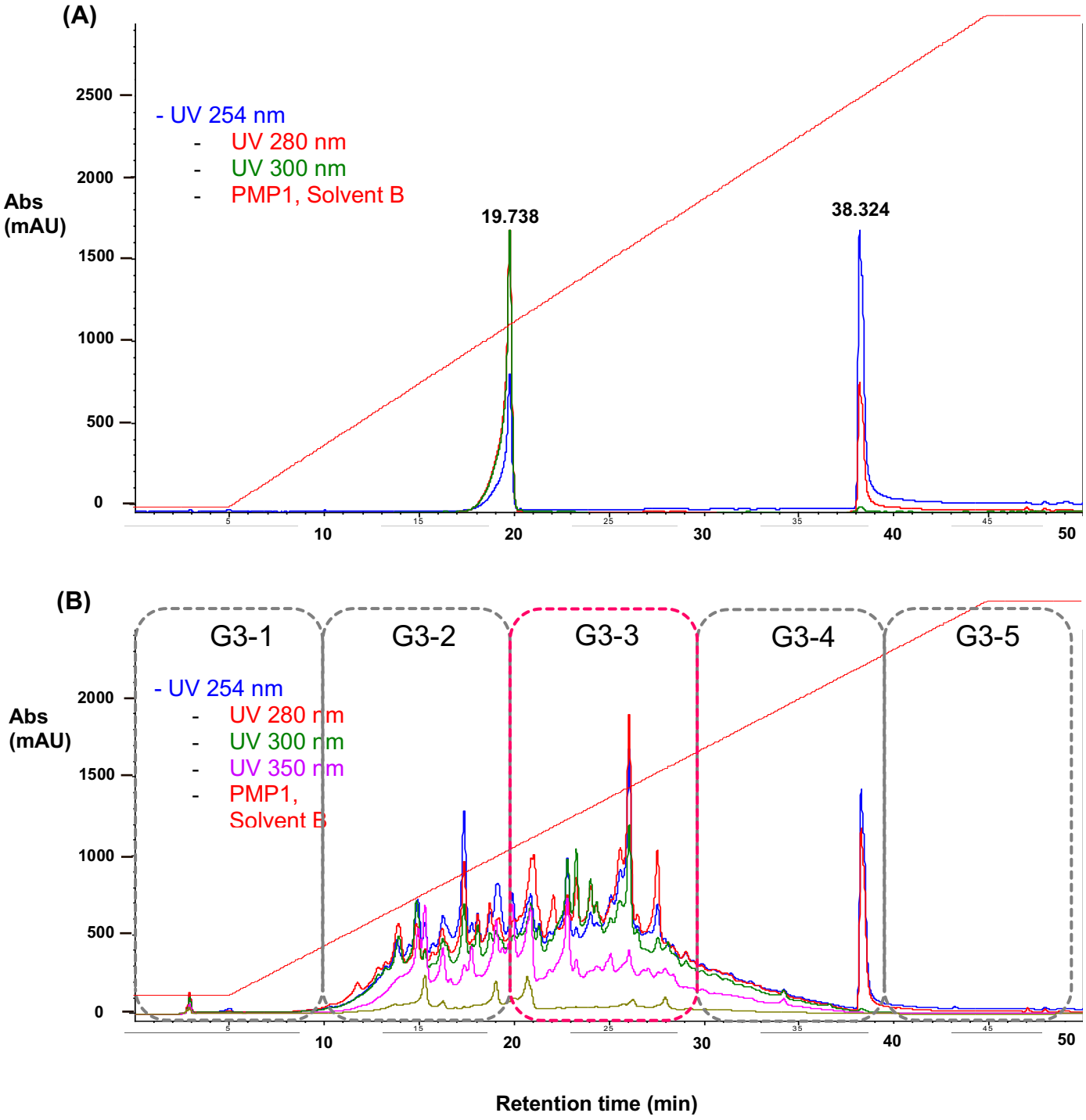

Figure 16. HPLC elution profile of glabridin (A) and licorice fraction G3 (B). The elution was separated in five fractions (10 min for each).

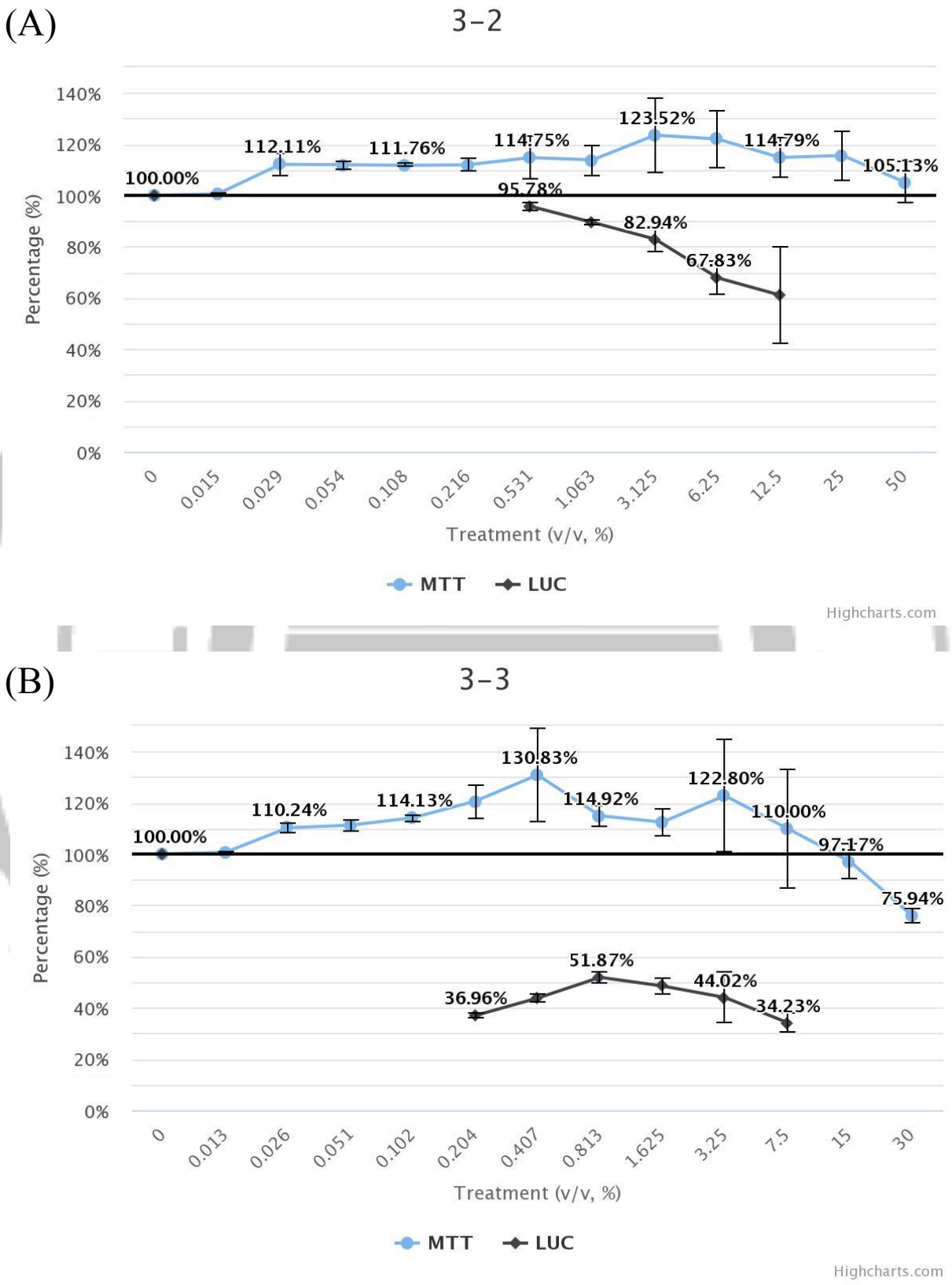

Figure 17. Effect of licorice fractions G3-2 and G3-3 on cell growth and luciferase activity in L8 cells.

DISCUSSION

Myostatin, is one of the major regulators of skeletal muscle development. It is a member of the transforming growth factor-β (TGF-β) superfamily. Myostatin plays a negative regulator in skeletal muscle growth. Overexpression of myostatin induces skeletal muscle atrophy and the mutations in the myostatin-encoding region are response for muscle hypertrophy and hyperplasia (Swatland and Kieffe, 1974). Passive vaccination and monoclonal antibody were used to increase animal growth and induced muscle hypertrophy (Bogdanovich *et al*., 2002; Liang *et al*., 2007). However, these methods were too time consuming and labor intensive. CMHs were used as daily health care or therapy in Asia for long time. Recently, more and more CMHs were added in animal feed to enhance animal growth. Unfortunately, usage of CMHs in animal growth does not have systemic analysis, so, it is important to establish a simple platform to screen the effective CMHs before using in animal feed.

Myostatin is one of major factor involved in muscle growth. Effective CMHs on regulation of myostatin gene expression are the candidate for animal growth enhancer. To establish a myostatin gene expression regulator screen system, mouse myostatin 5' regulatory region was inserted into pMetLuc2 plasmid (Figure 6). The plasmids were transfected onto L8 myoblasts and selected by G418. The expression of reporter gene, luciferase, in L8 myoblasts is under the control of myostatin 5'-regulatory region.

Twenty seven CMHs were screened by L8-myostatin molecular scanning system. Amount 27 CMHs, licorice, perilla, houttuynia cordata, and jiaogulan inhibited the activity of luciferase in transfected cells. In addition, the inhibition of luciferase activity is correlated with the enhancement of cell growth. These

results implied that these 4 CMHs promoted the L8 myoblast cell growth mediated by the inhibition of myostatin gene expression (Figure 8-9).

To confirm myostatin protein concentration is positive correlated with luciferase activity in transfected L8 cells, Western blot analysis was used. The transfected L8 cells were treated with licorice extract A (20 μg/mL) and B (10 μg/mL) for 24 h. The results showed that licorice A significantly decreased myostatin protein level. In addition, the luciferase activity was inhibited by Licorice A (Figure 10). The results imply that the luciferase activity is positive correlated with myostatin protein level (Figure 11). These results demonstrated that the luciferase expression through the pMetLuc2mMSTNPL plasmid in L8 cell can be the indicator of the myostatin protein level.

Licorice flavonoid oil (LFO) diet supplement significantly improved elderly body trunk muscle mass and body fat mass (Kinoshita *et al*., 2017). Recently, one of licorice major ingredient, glabridin, was found to inhibit dexamethasone-induced protein degradation to prevent C_2C_{12} myotubes and the muscle atrophy in mice (Yoshioka *et al*., 2019). Glabridin is antagonist of dexamethasone. It binds to glucocorticoid receptor to block the action of glucocorticoid. In this study, licorice ethanol extract inhibited the L8 myoblasts cell proliferation mediate by the inhibition of myostatin gene expression (Figure 8A). However, glabridin enhanced the L8 myoblast proliferation, but did not decrease the myostatin gene expression (Figure 14B). To identify the active ingredients in licorice, HPLC was used to perform the separation of licorice components. Enhancement of cell proliferation/inhibition of myostatin gene expression activities were identified in Fraction 3 (G3) (Figure 14A). In the chromatogram profile, G3 and glabridin are overlapped (Figure 12). To confirm the G3 active compound is not glabridin, G3 was applied to HPLC again. Licorice

fraction G3-2 and G3-3 increased transfected L8 cell growth, and inhibited luciferase activity in transfected L8 cell (Figure 17). The glabridin was applied into the same column with the same elution condition. The result showed that the retention time for glabridin is before 20 min (Figure 16A). This result implies that glabridin may contribute the effect of G3-2 on cell growth, while G3-3 contains other unknown component(s) affected the myoblast cell growth and luciferase activity.

In the future, identification of active ingredient in G3-3 of licorice will be carry on by LC-MS. Animal study will also be conducted. In addition, more CMHs will be screened by this molecular screening system to find more nature animal growth enhancer in CMHs.

REFERENCES

Aarestrup, F. M., F. Bager, N. E. Jensen, M. Madsen, A. Meyling, and H. C. Wegener. 1998. Surveillance of antimicrobial resistance in bacteria isolated from food animals to antimicrobial growth promoters and related therapeutic agents in Denmark. APMIS 106:606-622.

Ahn, J., H. Lee, J. Jang, S. Kim, and T. Ha. 2013. Anti-obesity effects of glabridin-rich supercritical carbon dioxide extract of licorice in high- fat-fed obese mice. Food Chem. Toxicol. 51:439-445.

Arifullah, M., N. D. Namsa, M. Mandal, K. K. Chiruvella, P. Vikrama, and G. R. Gopal. 2013. Evaluation of antibacterial and antioxidant potential of andrographolide and echiodinin isolated from callus culture of Andrographis paniculata Nees. Asian Pac. J. Trop. Biomed. 3:604-610.

Bataillé, L., I. Delon, J. P. Da Ponte, N. H. Brown, and K. Jagla. 2010. Downstream of identity genes: muscle-type-specific regulation of the fusion process. Dev. Cell 19:317-328.

Beyer, T.A., M. Narimatsu, A. Weiss, L. David, and J.L. Wrana. 2013 The TGFβ superfamily in stem cell biology and early mammalian embryonic development. Biophys. Acta-Gen. Subj.1830:2268-2279.

Bogdanovich, S., T. O. Krag, E. R. Barton, L. D. Morris, L. A. Whittemore, R. S. Ahima, and T. S. Khurana. 2002. Functional improvement of dystrophic muscle by myostatin blockade. Nature 420:418-421.

Bongiorni, S., F. Tilesi, S. Bicorgna, F. Iacoponi, D. Willems, M. Gargani, M. D. Andrea, F. Pilla, and A. Valentini. 2014. Promoter polymorphisms in genes involved in porcine myogenesis influence their transcriptional activity. BMC Genet. 15:119-126.

Bradford, M. M. 1976. Rapid and sensitive method for the quantitation of microgram quantities of protein utilizing the principle of protein-dye binding. Anal. Biochem. 72:248-254.

Castanon, J. I. R. 2007. History of the use of antibiotic as growth promoters in european poultry feeds Poult. Sci. 86:2466-2471.

Choi, A. Y., J. H. Choi, K. Y. Hwang, Y. J. Jeong, W. Choe, K. S. Yoon, J. Ha, S. S. Kim, J. H. Youn, E. J. Yeo, and I. Kang. 2014. Licochalcone a induces apoptosis through endoplasmic reticulum stress via a phospholipase cγ1-, Ca^{2+}-, and reactive oxygen species-dependent pathway in HepG2 human hepatocellular carcinoma cells. Apoptosis 19:682-697.

Choudhary, M., V. Kumar, H. Malhotra, and S. Singh. 2015. Medicinal plants with potential anti-arthritic activity. J. Intercult. Ethnopharmacol. 4:147-179.

Dastagir, G., and M. A. Rizvi. 2016. Review - *Glycyrrhiza glabra* . (liquorice). Pak. J. Pharm. Sci. 29:1727-1733.

Denizot, F., and R. Lang. 1986. Rapid colorimetric assay for cell growth and survival: Modifications to the tetrazolium dye procedure giving improved sensitivity and reliability. J. Immunol. Methods 89:271-277.

Deveaux, V., I. Cassar-Malek, and B. Picard. 2001. Comparison of contractile characteristics of muscle from Holstein and double-muscled Belgian Blue fetuses. Comp. Biochem. Physiol. A-Mol. Integr. Physiol. 131:21-29.

Dominique, J.-E., and C. Gérard. 2006. Myostatin regulation of muscle development: Molecular basis, natural mutations, physiopathological aspects. Exp. Cell Res. 312:2401-2414.

Fang, M., D. Zhu, C. Luo, C. Li, C. Zhu, J. Ou, H. Li, Y. Zhou, C. Huo, W. Liu, J. Peng, Q. Peng, and Z. Mo. 2018. In vitro and in vivo anti-malignant melanoma activity of Alocasia cucullata via modulation of the phosphatase and tensin homolog/phosphoinositide 3-kinase/AKT pathway. J. Ethnopharmacol. 213:359-365.

Franceschelli, S., M. Pesce, A. Ferrone, D. M. P. Gatta, A. Patruno, M. A. D. Lutiis, J. L. Quiles, A. Grilli, M. Felaco, and L. Speranza. 2017. Biological effect of licochalcone C on the regulation of PI3K/Akt/eNOS and NFκB/iNOS/NO signaling pathways in H9c2 cells in response to LPS stimulation. Int. J. Mol. Sci. 18:690-703.

Fuhrman, B., and M. Aviram. 2001. Flavonoids protect LDL from oxidation and attenuate atherosclerosis. Curr. Opin. Lipidology 12:41-48.

Fuhrman, B., S. Buch, J. Vaya, P. A. Belinky, R. Coleman, T. Hayek, and M. Aviram. 1997. Licorice extract and its major polyphenol glabridin protect low-density lipoprotein against lipid peroxidation: In vitro and ex vivo

studies in humans and in atherosclerotic apolipoprotein E-deficient mice. Am. J. Clin. Nutr. 66:267-275.

Gerrard, D. E., and M. D. Judge, 1993. Induction of myoblast proliferation in l6 myoblast cultures by fetal serum of double-muscled and normal cattle. J. Anim. Sci. 71:1464-1470.

Grassi, D., G. Desideri, and C. Ferri. 2010. Flavonoids: Antioxidants against atherosclerosis. Nutrients 2:889-902.

Hayashi, H., S. Tamura, R. Chiba, I, Fuji, N. Yoshikawa, I. Fattokho, and M. Saido. 2016. Field survey of *Glycyrrhiza* plants in Central Asia (4). Characterization of *G. Glabra* and *G. Bucharica* collected in Tajikistan. Biol. Pharm. Bull 39:1781-1786.

Hosseinzadeh, H., and M. Nassiri-Asl. 2015. Pharmacological effects of *Glycyrrhiza spp*. and its bioactive constituents: Update and review. Phytother. Res. 29:1868-1886.

Ji, B., L. Zhuo, B. Yang, Y. Wang, L. Li, M. Yu, Y. Zhao, and Z. Yu. 2017. Development and validation of a sensitive and fast uplcms/ms method for simultaneous determination of seven bioactive compounds in rat plasma after oral administration of guizhi-gancao decoction. J. Pharm. Biomed. Anal. 137:23-32.

Jiang, Y. L., N. Li, G. Plastow, Z. L. Liu, X. X. Hu, and C. X. Wu. 2002. Identification of three SNPs in the porcine myostatin gene (MSTN). Anim. Biotechnol. 13:173-178.

Jung, E. H., J. H. Lee, S. C. Kim, and Y. W. Kim. 2017. Ampk activation by liquiritigenin inhibited oxidative hepatic injury and mitochondrial dysfunction induced by nutrition deprivation as mediated with induction of farnesoid x receptor. Eur. J. Nutr. 56:635-647.

Kim, Y. S., N. K. Bobbili, Y. K. Lee, H. J. Jin, and M. A. Dunn. 2007. Production of a polyclonal anti-myostatin antibody and the effects of in ovo administration of the antibody on posthatch broiler growth and muscle mass. Poult. Sci. 86:1196-1205.

Kinoshita, T., A. Matsumoto, K. Yoshino, and S. Furukawa. 2017. The effects of licorice flavonoid oil with respect to increasing muscle mass: a randomized, double-blind, placebo-controlled trial. J. Sci. Food Agric. 97:2339-2345.

Kuang, Y., Y. Lin, K. Li, W. Song, S. Ji, X. Qiao, Q. Zhang, and M. Ye. 2017. Screening of hepatoprotective compounds from licorice against carbon tetrachloride and acetaminophen induced HepG2 cells injury. Phytomedicine 34:59-66.

Kuroda, M.,Y. Mimaki, S. Honda, H. Tanaka, S. Yokota, and T. Mae. 2010. Phenolics from Glycyrrhiza glabra roots and their PPAR-γ ligand-binding activity. Bioorg. Med. Chem. Lett. 18: 962-970.

Langley, B., M. Thomas, A. Bishop, M. Sharma, S.Gilmour, and R. Kambadur. 2002. Myostatin inhibits myoblast differentiation by down-regulating myoD expression J. Biol. Chem. 277:49831-49840.

Lach-Trifilieff, E., G. C. Minetti, K. Sheppard, C. Ibebunjo, J. N. Feige, S. Hartmann, S. Brachat, H. Rivet, C. Koelbing, F. Morvan, S. Hatakeyama, and D. J. Glass. 2014. An antibody blocking activin type II receptors induces strong skeletal muscle hypertrophy and protects from atrophy. Mol. Cell Biol. 34:606-618.

Lecomte, S., M. Lelong, G. Bourgine, T. Efstathiou, C. Saligaut, and F. Pakdel. 2017. Assessment of the potential activity of major dietary compounds as selective estrogen receptor modulators in two distinct cell models for proliferation and differentiation. Toxicol. Appl. Pharmacol. 325:61-70.

Lee, K. K., Y. Omiya, M. Yuzurihara, Y. Kase, and H. Kobayashi. 2013. Antispasmodic effect of shakuyakukanzoto extract on experimental muscle cramps in vivo: Role of the active constituents of glycyrrhizae radix. J. Ethnopharmacol. 145:286-293.

Lee S. J., and A.C. McPherron. 2001. Regulation of myostatin activity and muscle growth. Proc. Natl. Acad. Sci. U.S.A. 98:9306-931.

Liang, Y. C., J. Y. Yeh, and B. R. Ou. 2007. Effect of maternal myostatin antibody on offspring growth performance and body composition in mice. Eur. J. Exp. Biol. 210:477-483.

Liu, D., Q. Xu, L. Zang, S. Liang, Y. Wu, S. Wei, and Y. Jiang. 2010. Identification and genetic effect of haplotypes in the promoter region of porcine myostatin gene. Anim. Genet. 46:6-14.

Mahapatra, D. K., V. Asati, and S. K. Bharti. 2015. Chalcones and their therapeutic targets for the management of diabetes: Structural and pharmacological perspectives. Eur. J. Med. Chem. 92:839-865.

Manceau, M., J. Gros, K. Savage, V. Thomé, A. McPherron, B. Paterson, and C. Marcelle. 2008. Myostatin promotes the terminal differentiation of embryonic muscle progenitors. Genes Dev. 22:668-681.

McFarlane, C., B. Langley, M. Thomas, A. Hennebry, E. Plummer, G. Nicholas, C. McMahon, M. Sharma, and R. Kambadur. 2005. Proteolytic processing of myostatin is autoregulated during myogenesis. Dev. Biol. 283:58-69.

McPherron, A. C., and S. J. Lee. 1996. The transforming growth factor superfamily. In: D. Leroith, and C. Bondy, editors, Growth Factors, volume 1 of Growth Factors and Cytokines in Health and Disease. JAI press. p. 357-393.

Messier, C., and D. Grenier. 2011. Effect of licorice compounds licochalcone a, glabridin and glycyrrhizic acid on growth and virulence properties of candida albicans. Mycoses 54:e801-e806.

Millay, D. P., J. R. O'Rourke, L. B. Sutherland, S. Bezprozvannaya, J. M. Shelton, R. Bassel-Duby, and E. N. Olson. 2013. Myomarker is a membrane activator of myoblast fusion and muscle formation. Nature 499:301-305.

Molloy, S. S., E. D. Anderson, F. Jean, and G. Thomas. 1999. Bi-cycling the furin pathway: From TGN localization to pathogen activation and embryogenesis. Trends Cell Biol. 9:28-35.

Molloy, S. S., L. Thomas, J. K. V. Slyke, P. E. Stenberg, and G. Thomas. 1994. Intracellular trafficking and activation of the furin proprotein convertase: Localization to the TGN and recycling from the cell surface. EMBO J.13:18-33.

Pirruccello-Straub, M., J. Jackson, S. Wawersik, M. T. Webster, L. Salta, K. Long, W. McConaughy, A. Capili, C. Boston, G. J. Carven, N. K. Mahanthappa, K. J. Turner, and A. Donovan. 2018. Blocking extracellular activation of myostatin as a strategy for treating muscle wasting. Sci Rep. 8:1-15.

Reed, S.A., P. B. Sandesara, S. M. Senf, and A. R. Judge. 2012 Inhibition of FoxO transcriptional activity prevents muscle fiber atrophy during cachexia and induces hypertrophy. Faseb J. 26:987-1000.

Ren, S., M. Wu, J. Guo, W. Zhang, X. Liu, L. Sun, R. Holyst, S. Hou, Y. Fang, and X. Feng. 2015. Sterilization of polydimethylsiloxane surface with chinese herb extract: a new antibiotic mechanism of chlorogenic acid. Sci. Rep. 5:10464-10475.

Ríos, R., I. Carneiro, V. M. Arce, and J. Devesa. 2001. Myostatin regulates cell survival during C2C12 myogenesis. Biochem. Biophys. Res. Commun. 280:561-566.

Rizzato, G., E. Scalabrin, M. Radaelli, G. Capodaglio, and O. Piccolo. 2017. A new exploration of licorice metabolome. Food Chem. 221:959-968.

Sawada, K., Y. Yamashita, T. Zhang, K. Nakagawa, and H. Ashida. 2014. Glabridin induces glucose uptake via the ampactivated protein kinase pathway in muscle cells. Mol. Cell. Endocrinol. 393:99-108.

Shen, C. L. 2010. Association of single nucleotide polymorphisms in myostatin 5'-regulatory region with egg production in various breeds of chicken. Master thesis of Tunghai Univ., Taichung.

Simmler, C., J. R. Anderson, L. Gauthier, D. C. Lankin, J. B. McAlpine, S.-N. Chen, and G. F. Pauli. 2015. Metabolite profiling and classification of DNA-authenticated licorice botanicals. J. Nat. Prod. 78:2007-2022

Siracusa, L., A. Saija, M. Cristani, F. Cimino, M. Arrigo, D. Trombet, and G. Ruberto. 2011. Phytocomplexes from liquorice (*Glycyrrhiza glabra L.*) leaves—Chemical characterization and evaluation of their antioxidant, anti-genotoxic and anti-inflammatory activity. Fitoterapia 82:546-556.

Swatland, H. J., N. M. Kieffer. Fetal Development of the Double Muscled Condition in Cattle. J. Anim. Sci. 38:752-757.

Taylor, W. E., S. Bhasin, J. Artaza, F. Byhower, M. Azam, J. Darril H. Willard, J. Frederick C. Kull, and N. G. Cadavid. 2001. Myostatin inhibits cell proliferation and protein synthesis in c2c12 muscle cells. Am. J. Physiol.-Endocrinol. Metab. 280:e221-e228.

Thomas, M., B. Langley, C. Berry, M. Sharma, S. Kirk, J. Bass, and R. Kambadur. 2000. Myostatin, a negative regulator of muscle growth, functions by inhibiting myoblast proliferation. J. Biol. Chem. 275:40235-40243.

Tu, P. A., L. L. Lo, Y. C. Chen, C. C. Hsu, J. W. Shiau, E. C. Lin, R. S. Lin, and P. H. Wang. 2013. Polymorphisms in the promoter region of myostatin gene are associated with carcass traits in pigs. J. Anim. Breed Genet. 131:116-122.

Wang, Q., Y. Qian, Q. Wang, Y. Yang, S. Ji, W. Song, X. Qiao, D. Guo, H. Liang, and M. Ye. 2015. Metabolites identification of bioactive licorice compounds in rats. J. Pharm. Biomed. Anal. 115:515-522.

Wang, R., C. Y. Zhang, L. P. Bai, H. D. Pan, L. M. Shu, A. N. T. Kong, E. L. H. Leung, L. Liu, and T. Li. 2015. Flavonoids derived from liquorice suppress murine macrophage activation by up-regulating heme oxygenase-1 independent of nrf2 activation. Int. Immunopharmacol. 28:917-924.

Wei, C., H. Ren, L. Xu, L. Li, R. Liu, L. Zhang, F. Zhao, J. Lu, X. Zhang, and Lixin Du. 2015. Signals of Ezh2, Src, and Akt involve in myostatin-Pax7 pathways regulating the myogenic fate determination during the sheep myoblast proliferation and differentiation. PLoS One 10:e0120956.

Whittemore, L. A., K. Song, X. Li, J. Aghajanian, M. Davies, S. Girgenrath, J. J. Hill, M. Jalenak, P. Kelley, A. Knight, R. Maylor, D. OHara, A. Pearson, A. Quazi, S. Ryerson, X. Y. Tan, K. N. Tomkinson, G. M. Veldman, A. Widom, J. F. Wright, S. Wudyka, L. Zhao, and N. M. Wolfman. 2003.

Inhibition of myostatin in adult mice increases skeletal muscle mass and strength. Biochem. Biophys. Res. Commun. 300:965-971.

Wolfman, N. M., A. C. McPherron, W. N. Pappano, M. V. Davies, K. Song, K. N. Tomkinson, J. F. Wright, L. Zhao, S. M. Sebald, D. S. Greenspan, and S. J. Lee. 2003. Activation of latent myostatin by the BMP-1/tolloid family of metalloproteinases. Proc. Natl. Acad. Sci. U.S.A 100:15842-15846.

Yoshioka, Y., Y. Kubota, Y. Samukawa, Y. Yamashita, and H. Ashida. 2019. Glabridin inhibits dexamethasone-induced muscle atrophy. Arch. Biochem. Biophys. 664:157-166.

Yoshioka, Y., Y. Yamashita, H. Kishida, K. Nakagawa, and H. Ashida. 2018. Licorice flavonoid oil enhances muscle mass in KK-Ay mice. Life Sci. 205:91-96.

Zhang, F., B. Deng, J. Wen, K. Chen, W. Liu, S. Ye, H. Huang, S. Jiang, and Y. Xiong. 2015. PPARγ and MyoD are differentially regulated by myostatin in adipose-derived stem cells and muscle satellite cells. Biochem. Biophys. Res. Commun. 458:375-380.

Zhang, Q., A. A. Vashisht, J. O'Rourke, S. Y. Corbel, R. Moran, A. Romero, L. Miraglia, J. Zhang, E. Durrant, C. Schmedt, S. C. Sampath, and S. C. Sampath. 2017. The microprotein Minion controls cell fusion and muscle formation. Nat. Commun. 8:1-14.

Zhang, Q., and M. Ye. 2009. Chemical analysis of the chinese herbal medicine gan-cao (licorice). J. Chromatogr. A. 1216:1954-1969.